Quantum Exchange Coupling: A Hypersensitive Indicator of Weak Interactions

Roger Kuhlman,[†] Eric Clot,[‡,§] Claude Leforestier,[‡,§] William E. Streib,[†] Odile Eisenstein,*[‡,§] and Kenneth G. Caulton*[†]

Contribution from the Department of Chemistry and Molecular Structure Center, Indiana University, Bloomington, Indiana 47405-4001, and Laboratoire de Chimie Théorique, Bâtiment 490, Université de Paris-Sud, 91405 Orsay, France

Received February 24, 1997[⊗]

Abstract: $Os(H)_3ClL_2$ (L = P^iPr_3) forms a 1:1 adduct with L′ = PEt_3, NH_3, MeCN, acetone, methanol, and THF. The case L′ = PEt_3 permits the clearest identification of adduct structure as pentagonal bipyramidal. For NH_3 and MeCN, the respective kinetics of L′ loss are measured as $\Delta H^‡$ = 20.7(3) and 17.6(3) kcal/mol and $\Delta S^‡$ = 16(1) and 14.7(9) cal/(mol K). For acetone, methanol, and THF, the following respective $\Delta H°$ and $\Delta S°$ values for L′ binding are measured: $\Delta H°$ = −10.4(1), −6.66(8), and −5.8(2) kcal/mol; $\Delta S°$ = −41.8(5), −25.5(3), and −33(1) cal/(mol K). Decoalesced ^1H NMR spectra are reported for several of these $Os(H)_3ClL_2L′$ species, and they show a variety of examples of quantum exchange coupling among the hydride ligands. The values of J_{ex} are higher when L′ is a more weakly-binding ligand. The quantum exchange coupling constants of $Os(H)_3XL_2$ (X = Cl, Br, I, OCH_2CF_3, $OCH(CF_3)_2$) in CD_2Cl_2, in toluene, and in methylcyclohexane show an unprecedented decrease of J with increasing temperature, which is attributed to weak formation of $Os(H)_3Cl(solvent)L_2$ adducts at low temperature. For L′ = CO, adduct formation leads to liberation of coordinated H_2. Excess L′ = MeCN or NH_3 slowly leads to formation of $[Os(H)_3L′_2L_2]Cl$; the X-ray structure for L′ = NH_3 is reported. Crystal data (−171 °C): a = 11.561(4) Å, b = 14.215(5) Å, c = 8.851(3) Å, α = 97.51(2)°, β = 107.73(2)°, γ = 104.47(2)°, with Z = 2 in space group $P\bar{1}$. The potential energy was calculated for exchange of 2H of $OsH_3X(PH_3)_2L$ (X = Cl with L = no ligand and PH_3, X = I with L = no ligand) using effective core potential *ab initio* methods at the MP2 level. The site exchange is found to be energetically easier for Cl than for I, in agreement with experiment. The hydride site exchange in the seven-coordinate species $OsH_3Cl(PH_3)_3$ (a model for coordination of either ligand or solvent to Os) is found to be easier than that in the 16-electron species. No dihydrogen ligand is located on the reaction path for site exchange. The current theory which relates quantum exchange to a tunneling effect was used for calculating J_{ex} as a function of temperature. The dynamic study was done using several sets of coordinates, in particular the rotation angle ϕ and the internuclear distance r between the exchanging H. The vibrational levels have been calculated and the symmetry of each level assigned within the permutation group in order to determine the nature of the nuclear spin function associated with each level. It is found that the rotation, ϕ, gives rise to the largest tunneling effect but that r cannot be neglected. The influence of the temperature, $J_{ex}(T)$, was included by a Boltzmann distribution. The results are in qualitative agreement with experiment in that quantum exchange coupling is larger in the case of Cl than in the case of I. Additional ligand L increases the value of the quantum exchange coupling mostly by lowering the activation energy for pairwise exchange.

Introduction

The discovery[1] of unusually large splittings in the energy levels of multiple (>2) chemically-inequivalent hydrogen nuclei, measurable by ^1H NMR spectroscopy, has sparked much activity to experimentally characterize and theoretically model the phenomenon which is now called quantum exchange coupling (QEC).[2−17] The associated ^1H NMR spectra follow exactly the rules of "traditional" NMR energy states and selection rules[4] but with larger than normal (sometimes immensely larger) coupling constants, J. These J values do not arise from Fermi

contact or other traditional "magnetic" mechanisms, and, indeed, they have nothing to do with shared electron density, s orbital character, or structural parameters such as interbond angle. Two *seemingly* disparate models have been offered to model the QEC phenomenon. Both involve exchange of inequivalent hydrogen

---

[†] Indiana University.

[‡] Université de Paris-Sud.

[§] Present address: LSDSMS (UMR 5636), Case Courrier 14, Université de Montpellier 2, 34095 Montpellier Cedex 5, France.

[⊗] Abstract published in *Advance ACS Abstracts,* October 1, 1997.

(1) (a) Arliguie, T.; Chaudret, B.; Devillers, J.; Poilblanc, R. *C. R. Acad. Sci. Paris* **1987**, *305II*, 1523. (b) Antinolo, A.; Chaudret, B.; Commenges, G.; Fajardo, M.; Jalon, F.; Morris, R. H.; Otero, A.; Schweitzer, C. T. *J. Chem. Soc., Chem. Commun.* **1988**, 1210. (c) Heinekey, D. M.; Payne, N. G.; Schulte, G. K. *J. Am. Chem. Soc.* **1988**, *110*, 2303.

(2) (a) Jones, D. H.; Labinger, J. A.; Weitekamp, D. P. *J. Am. Chem. Soc.* **1989**, *111*, 3087. (b) Zilm, K. W.; Heinekey, D. M.; Millar, J. M.; Payne, N. G.; Demou, P. *J. Am. Chem. Soc.* **1989**, *111*, 3088.

(3) (a) Heinekey, D. M.; Millar, J. M.; Koetzle, T. F.; Payne, N. G.; Zilm, K. W. *J. Am. Chem. Soc.* **1990**, *112*, 909. (b) Zilm, K. W.; Heinekey, D. M.; Millar, J. M.; Payne, N. G.; Neshyba, S. P.; Duchamp, J. C.; Szczyrba, J. *J. Am. Chem. Soc.* **1990**, *112*, 920. (c) Heinekey, D. M.; Payne, N. G.; Sofield, C. D. *Organometallics* **1990**, *9*, 2643.

(4) Zilm, K. W.; Millar, J. M. *Adv. Magn. Reson.* **1990**, *15*, 163.

(5) (a) Arliguie, T.; Chaudret, B.; Jalón, F.; Otero, A.; López, J. A.; Lahoz, F. J. *Organometallics* **1991**, *10*, 1888. (b) Heinekey, D. M.; Harper, T. G. P. *Organometallics* **1991**, *10*, 2891. (c) Heinekey, D. M. *J. Am. Chem. Soc.* **1991**, *113*, 6074.

(6) Barthelat, J. C.; Chaudret, B.; Daudey, J. P.; DeLoth, P.; Poilblanc, R. *J. Am. Chem. Soc.* **1991**, *113*, 9896.

(7) (a) Antiñolo, A.; Carrillo, F.; Fernández-Baeza, J.; Otero, A.; Fajardo, M.; Chaudret, B. *Inorg. Chem.* **1992**, *31*, 5156. (b) Chaudret, B.; Limbach, H. H.; Moise, C. *C. R. Acad. Sci. Ser. II* **1992**, *315*, 533.

(8) (a) Limbach, H. H.; Scherer, G.; Maurer, M.; Chaudret, B. *Angew. Chem., Int. Ed. Engl.* **1992**, *31*, 1369. (b) Inati, S. J.; Zilm, K. W. *Phys. Rev. Lett.* **1992**, *68*, 3273.

(9) (a) Jarid, A.; Moreno, M.; Lledós, A.; Lluch, J. M.; Bertrán, J. *J. Am. Chem. Soc.* **1993**, *115*, 5861. (b) Hiller, E. M.; Harris, R. A. *J. Chem. Phys.* **1993**, *98*, 2077; **1993**, *99*, 7652.

nuclei. One[8] proposes that a thermal equilibrium exists between the ground state structure (inequivalent hydrides) and a dihydrogen isomer, whose function is to exchange the two inequivalent hydrogen nuclei. Purely quantum mechanical studies have been carried out. One model[9,15] is built on the mechanism proposed by Limbach et al.[8] and assumes a reaction path going through a dihydrogen structure. The other model[13] focuses on the characterization of the symmetry properties associated with the exchange mechanism. The potential energy barrier is most conducive to QEC (we shall see) if it involves only the motion of H, the lightest nucleus. The structure at the barrier maximum *may* involve an H_2 ligand but does not require one, and an H_2 ligand is in no way central to this theoretical model. Common to the two theories is the need for a "low" energy barrier, i.e., *any* second structure which has energy not too far above the ground state.

One of the early models for QEC was derived from the Landesman model[6,18] used to study exchange phenomena in liquid helium. The model of Landesman suffers from several approximations: (i) In this model, particles are considered as hard spheres. The exchange motion involves an in-plane motion of the nuclei, and no reference is made to the shape of the potential energy surface and, in particular, to the height of the barrier for exchange. (ii) The symmetry under permutation of the two hydrides which is central to the theory established by Zilm is not referenced in the Landesman model. (iii) The exchange is calculated using only the vibrational ground state, while a proper study should take into account all the vibrational states below the barrier. Later dynamics studies[9,13,15] have taken into account part or all of the above aspects.

The characteristic observed properties of the QEC coupling constant which must be explained by any theory are the following:

(1) J can be large.

(2) J increases as temperature increases.

(3) J increases as electron-withdrawing substituents are incorporated into a molecule (this has been used to support the idea that a thermally-accessible H_2 complex is involved in the QEC phenomenon). In $Cp_2M(H)_3$, cationic or neutral, J also increases from W to Mo[5c] and from Ta to Nb[5c,6] (easier to reduce and thus achieve $M(H_2)$).

(4) Only two H nuclei are sufficient to give rise to the phenomenon[12b−d] (this is important, since all of the early

examples of QEC involved $L_nM(H)_3$ species, which might have led to the conclusion that three H's are the necessary minimum unit for QEC). The J(AA) coupling constant does not influence the normal NMR spectrum of a spin system of n magnetically equivalent nuclei, A_n. Consequently, determination of the H/H coupling constant of a metal dihydride complex $L_nM(H)_2$ (without recourse to partial deuteration) requires asymmetry in the L_nM substructure to make the two hydrides inequivalent. It is for this reason that quantum exchange coupling was first discovered in the AM_2 spin system of C_s- or C_2-symmetric L_nM-$(H)_3$ molecules. Subsequent observations[12b−d] of exchange coupling in MH_2 species have confirmed that the occurrence of quantum exchange coupling is in no way limited to or favored by $L_nM(H)_3$ species.

(5) No purely organic or main group compound has shown QEC.

(6) Some $L_nM(^aH)(^bH)$ compounds with inequivalent hydrides show only magnetic couplings (ordinary magnitude).

Despite these fascinating aspects, the potential of these tremendous coupling constants in chemical observations has been little utilized. Since exchange couplings are often orders of magnitude larger than magnetic H/H coupling constants, QEC offers possibilities for recognition of unfavorable species in equilibria and for accurate structural characterization.

We have reported the first unsaturated molecules which show exchange coupling, $Os(H)_3X(P^iPr_3)_2$.[11] We have reported in detail the complicated site exchange (fluxionality) of the H_2 adduct of these molecules, $Os(H)_3X(H_2)(P^iPr_3)_2$, and the highly selective exchange coupling which occurs there.[17] Since these saturated molecules have a structure (**I**, $L' = H_2$) which destroys the C_{2v} symmetry of $Os(H)_3X(P^iPr_3)_2$, there are, in principle, three H/H coupling constants observable among the hydrides of **I**. Breaking the symmetry of the AM_2 spin system with L'
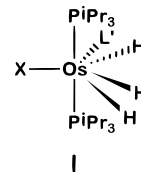
makes it possible to establish the *selectivity* of exchange coupling. We report here a study of a wide variety of adducts of type **I** and the consequences of systematically varying L' on exchange coupling among these three hydrides. Because of the relatively large values of the exchange coupling, these become a hypersensitive probe of even very weak interactions with unconventional donors L', including hydrocarbons.

Results

Synthesis and Structure of $(P^iPr_3)_2OsH_3X$ (X = Cl, 1; Br, 2; I, 3; $OCH(CF_3)_2$, 4; OCH_2CF_3, 5). Complexes **1−3** are synthesized via dehydrohalogenation by reaction of $L_2OsH_2X_2$ with H_2 in the presence of NEt_3 (eqs 1 and 2). The monohalide

(10) (a) Antiñolo, A.; Carrillo, F.; Chaudret, B.; Fajardo, M.; Fernández-Baeza, J.; Lanfranchi, M.; Limbach, H. H.; Maurer, M.; Otero, A.; Pellinghelli, M. A. *Inorg. Chem.* **1994**, *33*, 5163. (b) Heinekey, D. M.; Oldham, W. J. *J. Am. Chem. Soc.* **1994**, *116*, 3137. (c) Miller, E. M.; Harris, R. A. *J. Chem. Phys.* **1994**, *100*, 2522. (d) Szymanski, S. *J. Mol. Struct.* **1994**, *321*, 115.

(11) Gusev, D. G.; Kuhlman, R.; Sini, G.; Eisenstein, O.; Caulton, K. G. *J. Am. Chem. Soc.* **1994**, *116*, 2685.

(12) (a) Jarid, A.; Moreno M.; Lledós, A.; Lluch, J. M.; Bertrán, J. *J. Am. Chem. Soc.* **1995**, *117*, 1069. (b) Sabo-Etienne, S.; Chaudret, B.; Abou el Makarim, H.; Barthelat, J.-C.; Daudey, J.-P.; Ulrich, S.; Limbach, H.-H.; Moise, C. *J. Am. Chem. Soc.* **1995**, *117*, 11602. (c) Jalón, F. A.; Otero, A.; Manzano, B. R.; Villasenor, E.; Chaudret, B. *J. Am. Chem. Soc.* **1995**, *117*, 10123. (d) Antiñolo, A.; Carrilo-Hermosilla, F.; Chaudret, B.; Fajardo, M.; Fernandez-Baeza, J.; Lanfranchi, M.; Limbach, H. H.; Maurer, M.; Otero, A.; Pellinghelli, M. A. *Inorg. Chem.* **1996**, *35*, 7873. (e) Wiedenbruch, R.; Schick, M.; Pampel, A.; Meier, B. H.; Meyer, R.; Ernst, R. R.; Chaloupka, S.; Venanzi, L. M. *J. Phys. Chem.* **1995**, *99*, 13088. (f) Scheurer, C.; Wiedenbruch, R.; Meyer, R.; Ernst, R. R.; Heinekey, D. M. *J. Chem. Phys.* **1997**, *106*, 1.

(13) Clot, E.; Leforestier, C.; Eisenstein, O.; Pélissier, M. *J. Am. Chem. Soc.* **1995**, *117*, 1797.

(14) Heinekey, D. M.; Hinkle, A. S.; Close, J. D. *J. Am. Chem. Soc.* **1996**, *118*, 5353.

(15) Camanyes, S.; Maseras, F.; Moreno, M.; Lledós, A.; Lluch, J. M.; Bertrán, J. *J. Am. Chem. Soc.* **1996**, *118*, 4617.

(16) Szymanski, S. *J. Chem. Phys.* **1996**, *104*, 8216.

(17) Kuhlman, R.; Gusev, D. G.; Eisenstein, O.; Caulton, K. G., submitted for publication.

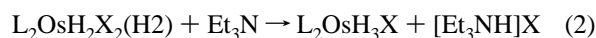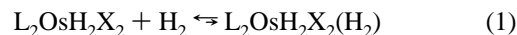(18) Landesman, A. *Ann. Phys. (Fr.)* **1973**, *8*, 53.

complexes weakly bind H_2, so removal of volatiles *in vacuo* also releases H_2 from the pentahydride complexes. They are generally isolated as oily brown solids and are very difficult to purify. The two alkoxide complexes (R = $CH(CF_3)_2$, **4**; CH_2-CF_3, **5**) are easily prepared by metathesis (TlOR) from the chloride complex (eq 3). The $M(H)_3$ substructure of these

$$L_2OsH_2X_2 + H_2 \rightleftarrows L_2OsH_2X_2(H_2) \qquad (1)$$

$$L_2OsH_2X_2(H2) + Et_3N \rightarrow L_2OsH_3X + [Et_3NH]X \qquad (2)$$

$$L_2Os(H)_3Cl + TlOR \rightarrow L_2Os(H)_3OR + TlCl \qquad (3)$$

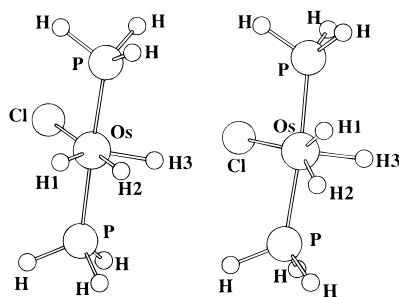**Figure 1.** Optimized structures of the ground state (left) and transition state (right) for H1/H2 exchange in $OsH_3Cl(PH_3)_2$.

complexes is quite similar to those of the $CpRu(PR_3)(H)_3$, $CpIr(PR_3)(H)_3^+$, and $Cp_2Nb(H)_3$ complexes known to exhibit exchange coupling.

The large J_{PP} of 274 Hz in $L_2Os(H)_3[OCH(CF_3)_2]$ (*trans* PR_3's) is measured directly (*vide infra*), and provides good evidence that the PR_3 ligands are *trans* (**II**). The H···H

II
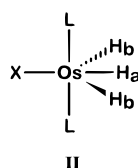
separations are determined by T_{1min} measurements of the hydride ligands. In $L_2Os(H)_3[OCH(CF_3)_2]$, two hydride resonances are observed below −30 °C. At −70 °C, T_{1min} values are measured separately for each of the two hydride signals. From these values, we can determine the relaxation rate constant due to hydride dipole−dipole interactions (R_{HH}) and that due to all other relaxation contributors (R^*) by using eqs 4 and 5, where

$$R_a = R^* + 2R_{HH} = 21.41 \text{ s}^{-1} \quad (4)$$

$$R_b = R^* + R_{HH} = 12.24 \text{ s}^{-1} \quad (5)$$

$$\therefore R_{HH} = 9.17 \text{ s}^{-1}, \quad R^* = 3.07 \text{ s}^{-1}$$

$R_a = 1/T_{1min}$ for the H_a resonance and $R_b = 1/T_{1min}$ for the H_b resonance (**II**). Solving for R^* and R_{HH} yields the values above. From this R_{HH}, an $H_a \cdots LH_b$ separation of 1.55 Å is calculated. The hydrides in L_2OsH_3X (X = Cl, **1**; Br, **2**; I, **3**) are all coalesced at their T_{1min} temperatures so that only an averaged T_{1min} can be observed. Using the same R^* (3.07 s^{-1}) for the halide complexes **1**−**3** (all have T_{1min} = 72(2) ms), a slightly longer $H_a \cdots H_b$ separation (1.59 Å) is calculated. The shorter H···H separation (smaller H−Os−H angle) in **4** is consistent with known trends in ligand X π-donor ability.[19] The better π-donor (alkoxide better than halide) leads to a greater distortion.

Structures and Bonding of $OsH_3X(PH_3)_2$ (X = Cl, I, OH) in Their Ground States. The results of the HF and MP2 geometry optimization with no symmetry constraints (C_1 point group) gives a structure which has essentially C_{2v} symmetry (Figure 1, Table 1) with Cl, Os, and the three H in the Π_0 plane, to which the Os−P bonds are essentially perpendicular. The Hessian, calculated only at the RHF level, indicates that this structure is a minimum. The absence of any negative eigenvalues in the updated Hessian matrix during the optimization procedure at the MP2 level suggests that the optimized structure is a true minimum. Equivalent results have been obtained for X = I.

The most important features of the experimental results are reproduced. For comparison, the average Os−H distance is

(19) Caulton, K. G. *New J. Chem.* **1994**, *18*, 25.

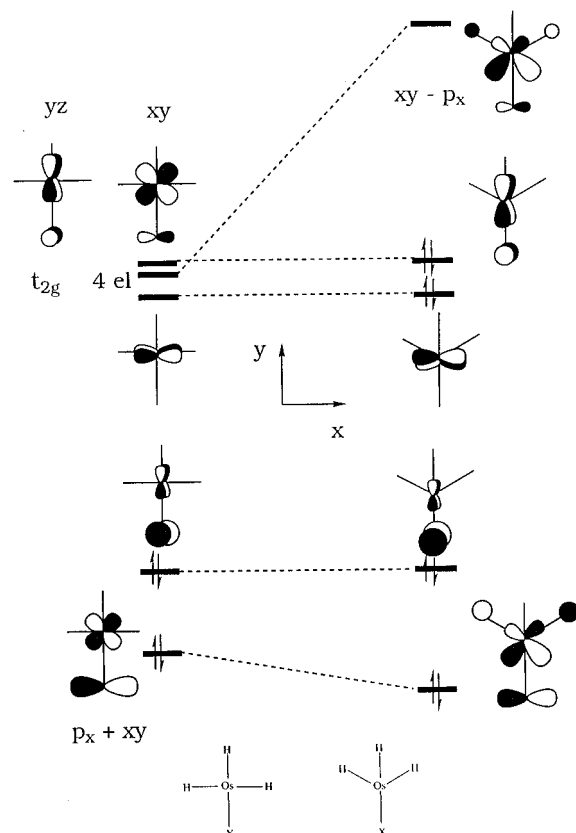**Figure 2.** Correlation diagram for decreasing the H−Os−H angles from 90° in OsH_3Xl_2 (the L ligands lie out of the plane of the drawing and are not shown).

slightly longer than that in $OsH_5L_3^+$, at 1.63 Å.[20] The Os−P bond length (2.29 Å) compares well to the experimental value of 2.3 Å for other 16-electron complexes like $OsH_2Cl_2(P^iPr_3)_2$[21] and $OsDCl_3(P^iPr_3)_2$.[22] The calculated Os−Cl bond (2.37 Å) is longer than the corresponding experimental value of the Os−Cl bond *trans* to D in $OsDCl_3(P^iPr_3)_3$ but shorter than the two other Os−Cl bonds. The most remarkable feature of the complex is in the acute *cis* H1(3)−Os−H2 angle. The calculated value of 57° is in excellent agreement with the experimental value of 60°. The other angular parameters are not remarkable.

An acute angle of 60° was found between the bulky phosphines and the *cis* deuterium in $OsDCl_3L_2$,[22] revealing that the analogous distortion is not due to a mutual attraction of the hydrides in OsH_3ClL_2 or to some steric constraints.

In the case of a d^4 electron count, an octahedral structure is unfavorable since the t_{2g} nonbonding orbitals would be only partially occupied.[23,24]

A correlation diagram (Figure 2) between the hypothetical octahedral structure (perpendicular phosphines not shown) and the observed structure indicates the origin of the stabilization upon decrease of the angle between the three hydrides. Two of the orbitals, yz and xz (z perpendicular to the Cl−Os−H plane), of the formal t_{2g} set of the octahedron are not affected because the change in the α (H1(3)−Os−H2) angle occurs in the nodal plane of these orbitals. In contrast, the two outside hydrogens, H1 and H3, overlap better with xy as α decreases,

(20) Johnson, T. J.; Albinati, A.; Koetzle, T. F.; Ricci, J.; Eisenstein, O.; Caulton, K. G. *Inorg. Chem.* **1994**, *32*, 4966.

(21) Aracama, M.; Esteruelas M. A.; Lahoz, F. J.; Lopez, J. A.; Meyer, U.; Oro, A.; Werner, H. *Inorg Chem.* **1991**, *30*, 288.

(22) Kuhlman, R.; Gusev, D. G.; Eremenko, I. L.; Berke, H.; Huffman, J. C.; Caulton, K. G. *J. Organomet. Chem.* **1997**, *536*, 139.

(23) Kubácek, P.; Hoffmann, R. *J. Am. Chem. Soc.* **1981**, *103*, 4320.

(24) Gusev, D. G.; Kuhlman, R.; Rambo, J. R.; Berke, H.; Eisenstein, O.; Caulton, K. G. *J. Am. Chem. Soc.* **1995**, *117*, 281.

Table 1. Optimized Distances (Å) and Angles (deg) of Os(H)₃X(PH₃)ₙ (X = Cl, I, and OH; n = 2; X = Cl, n = 3) in the Ground State (GS) and Transition State (TS) for H1/H2 Exchange

	n = 2					n = 3	
	X = Cl (GS)	X = Cl (TS)	X = I (GS)	X = I (TS)	X = OH (GS)	X = Cl (GS)	X = Cl (TS)
Os−H1	1.566	1.589	1.568	1.584	1.574	1.594	1.593
Os−H2	1.600	1.589	1.589	1.584	1.623	1.589	1.594
Os−H3	1.566	1.561	1.568	1.563	1.574	1.610	1.621
H1···H2	1.510	1.381	1.520	1.341	1.538	1.591	1.376
H2···H3	1.510	1.885	1.520	1.914	1.538	1.666	2.172
Os−X	2.374	2.371	2.674	2.694	2.010	2.487	2.470
Os−P	2.293	2.316	2.315[a]	2.315[a]	2.279[b]	2.280[c]/2.400[d]	2.285[c]/2.365[d]
H1−Os−H2	56.9	51.5	57.5	50.1	57.5	59.9	51.2
H2−Os−H3	56.9	73.5	57.5	74.9	57.5	62.8	85.0
H1−Os−X	122.9	128.4	120.9	148.1	122.5	83.7	89.2
P−Os−P	176.4	175.4	174.8	173.6	175.2	178.2	163.1
X−Os−P	91.8	87.6	92.6	86.8	98.6[b]	90.9[c]/76.4[d]	81.6[c]/92.6[d]

[a] Fixed value. [b] Value given for P *cis* to H of OH. For P *trans* to OH, Os−P = 2.303, P−Os−X = 86.1, Os−OH = 114.6. [c] P3. [d] P14.
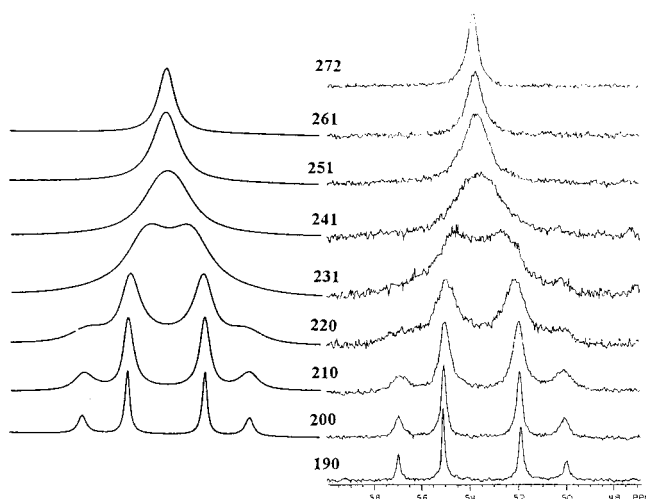
Figure 3. Simulated (left) and observed variable temperature (K) ³¹P{¹H} NMR spectra of (PⁱPr₃)₂Os(H)₃[OCH(CF₃)₂].

which stabilizes the bonding combination of the hydrides and $xy + p_x$. The $xy + p_x$ orbital also increases its overlap with the p_x Cl orbital via an additional mixing of the Os p_x orbital to make an Os−Cl π-bond. Since the LUMO is the out-of-phase combination of xy and the s orbitals of the H centers, moving α away from 90° raises its energy. The resulting geometry is, therefore, well adapted to a d⁴ electron count since it has only two d orbitals at low energy. The empty metal xy orbital is used for bonding the two outside hydrides and also for better interacting in a π fashion with one of the lone pair of Cl (p_x). The two other d orbitals, xz and yz, are not capable of any additional bonding since they are doubly-occupied. This accounts for the shorter outside Os−H bonds compared to the unique longer central Os−H bond and for π-bonding with X which shortens the Os−X distance.

The same reasoning on OsDCl₃(PH₃)₂ shows that the diminution of the P−Os−D angle permits better Os−P σ-bonds and a stronger π-bonding to the Cl *trans* to D (the shorter Os−Cl bond in the molecule, despite the *trans* influence of D). The ligands supporting the acute angle have the highest *trans* influence (H *vs* phosphine in the trihydride species, phosphine *vs* Cl in the trichloro complex). Moving away from a *trans* geometry is thus stabilizing.

The above distortions can only occur in 16-electron complexes and partially cancel the electron deficiency at the metal. The metal receives additional electron density from the hydrides via stronger σ-bonds and from one lone pair of X via a π-bond. The features are common to several electron-deficient complexes, even with very different shapes (e.g., OsH₂Cl₂L₂).[24]

The calculations on OsH₃(OH)(PH₃)₂ give a similar structure (Table 1) and show a preference for the OsO−H bond to eclipse Os−P, thus opposing steric preferences. This result is in accord with the use of the pure p orbital on the oxygen for π-bonding with the empty Os xy orbital. A similar result was obtained in related 16-electron Ir(III) complexes.[25]

Restricted Rotation about Os−O in L₂Os(H)₃(OR). The prediction from the calculations is confirmed by variable-temperature ³¹P NMR spectroscopy of **4**. The π-bond with the pure p lone pair of oxygen in **4** should hold the CH(CF₃)₂ group out of the equatorial plane of the molecule (see **III**), making the two phosphines inequivalent. Fast rotation around the Os−O
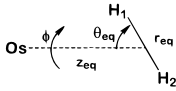

III
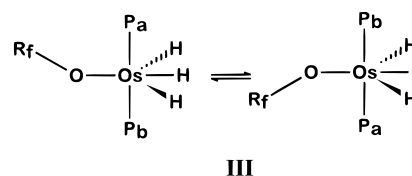
bond gives a single time-averaged ³¹P signal at room temperature. Cooling a toluene-d_8 solution of **4** causes ³¹P decoalescence to an AB pattern as this rotation is slowed. The Os−O π-bond is sufficient to make the sterically inferior structure the observed ground state. Shown in Figure 3 are simulated and experimental variable-temperature ³¹P NMR spectra for **4**. From the rate constants (see Supporting Information) obtained by the DNMR5 simulations, Eyring analysis yields the activation parameters $\Delta H^{\ddagger}$ = 7.1(3) kcal/mol and $\Delta S^{\ddagger}$ = −13(1) cal/(mol K) for rotation about the Os−O bond.

This value of $\Delta H^{\ddagger}$ (7 kcal/mol) is a rough estimate for the strength of the π-bond between Os and O. Because some π donation may also be present in the transition state (from the hybridized lone pair), the π-bond strength may slightly exceed the rotational barrier. However, the R group on the alkoxide is quite large, and rotation may require molecular deformations (such as narrowing the P−Os−P angle) which contribute to $\Delta H^{\ddagger}$. Thus, this $\Delta H^{\ddagger}$ could *over*estimate the π-bond strength.

The ³¹P signal for L₂OsH₃(OCH₂CF₃) (**5**) remains a singlet down to −90 °C in toluene-d_8 (line width = 66 Hz), which probably indicates that alkoxide rotation is faster for this smaller R group. No kinetic information is gained from *lack* of decoalescence, however, since the difference in chemical shift is unknown. Similarly, no ³¹P decoalescence is observed in **1** at −90 °C in toluene-d_8, which shows that the decoalescence seen for **4** is not due to some other process such as hindered rotation about Os−P or P−C bonds.

(25) Lunder, D. M.; Lobkovsky, E. B.; Streib, W. E.; Caulton, K. G. *J. Am. Chem. Soc.* **1991**, *113*, 1837.

Table 2. Optimized Structural Parameters and Relative Energy, E_{eq} (kcal/mol), of the Os$-$H1$-$H2 Unit Leading to Figure 4 (X = Cl)


ϕ	E_{eq}	r_{eq}	θ_{eq}	z_{eq}
0.0	0.0	1.509	88.54	1.391
10.0	+0.056	1.516	88.60	1.388
35.0	+2.492	1.522	89.20	1.381
50.0	+6.172	1.473	89.68	1.395
65.0	+9.990	1.403	90.04	1.416
75.0	+11.817	1.363	90.10	1.427
85.0	+12.772	1.342	90.05	1.433
90.0	+12.892	1.336	90.0	1.434

**Dependence of J on Activation Parameters and H$\cdots$H Separations. (a) Experiment.** As stated above, there are several factors which influence J_{ex}. At least two relevant parameters are experimentally measurable: $\Delta G^{\ddagger}$ for the site exchange and the H$-$H separation. According to tunneling theory, J_{ex} should increase with decreased H$-$H separation, and J_{ex} should increase with decreasing $\Delta G^{\ddagger}$ for the site exchange which permutes the two hydrogens. The complex (P^{i}Pr$_3$)$_2$OsH$_3$-[OCH(CF$_3$)$_2$] (**4**), which has a *shorter* H$-$H separation than (P^{i}Pr$_3$)$_2$OsH$_3$X (X = Cl, **1**; Br, **2**; I, **3**) also has a *smaller* coupling constant. Complex **4** also has a *higher* barrier to hydride site exchange ($\Delta H^{\ddagger} = 10.8(3)$ kcal/mol) than **1**$-$**3** ($\Delta H^{\ddagger} \approx 8-9$ kcal/mol). Complex **5**, (P^{i}Pr$_3$)$_2$Os(H)$_3$(OCH$_2$CF$_3$), has $\Delta H^{\ddagger} = 9.5(2)$ kcal/mol for the site exchange but the lowest coupling constant of all. The H/H coupling in **5** is only 33.5 Hz in toluene-d_8. Eyring plots for determination of these activation barriers to H$-$H site exchange in **4** and **5** were prepared from the rate constants (DNMR5) given in Supporting Information. The activation barriers for **1**$-$**3** were determined by single-point simulations of spectra at -60 °C in toluene-d_8, assuming J to be the same as that observed at -110 °C, and $\Delta S^{\ddagger} = 0$. Within the series **1**$-$**5**, we observe no consistent correlation of J with either H$-$H distance or $\Delta H^{\ddagger}$.

(b) Theory. The two permuting atoms are H1 and H2. Under the hypothesis of a correlated motion of the two hydrides, the transition state for the exchange has the dihedral angle ϕ between the plane H1$-$Os$-$H2 and Π_0 equal to 90°. This geometry, optimized with fixed $\phi = 90°$, was calculated to be 12.7 kcal$\cdot$mol^{-1} above the minimum (Figure 1, Table 1). The most important geometrical features of the ground state are maintained. The complex has essentially C_s symmetry with H3$-$Os$-$Cl as a mirror plane. The changes with respect to the ground state are of minor magnitude, with the exception of the nonbonding distance between H1 and H2 which decreases from 1.51 Å when $\phi = 0$ to 1.38 Å when $\phi = 90°$. However, this does not indicate the formation of an H$_2$ ligand since there is no accompanying significant increase in the Os$-$H1 and Os$-$H2 distances. It is also to be noted that H3 does not get closer to H1 and H2 so that there is no (H$_3$) species formed. While no Hessian was calculated for this structure, it is likely to be a transition state since (i) the updated Hessian has only positive eigenvalues for fixed value of ϕ, (ii) the gradient for ϕ is essentially zero, and (iii) the energy lowers when ϕ departs from 90°.

Reaction Coordinate for H1-H2 Exchange. Two variables, ϕ and θ (Table 2), can be used to describe the exchange of H1 and H2 since a transformation $\phi \rightarrow \phi + \pi$ and $\theta \rightarrow \pi - \theta$ interchanges two equivalent configurations. It is intuitive that changing ϕ is energetically more feasible than changing θ. Thus, describing the entire potential energy surface as a function of ϕ is appealing for the calculations. However, this model can
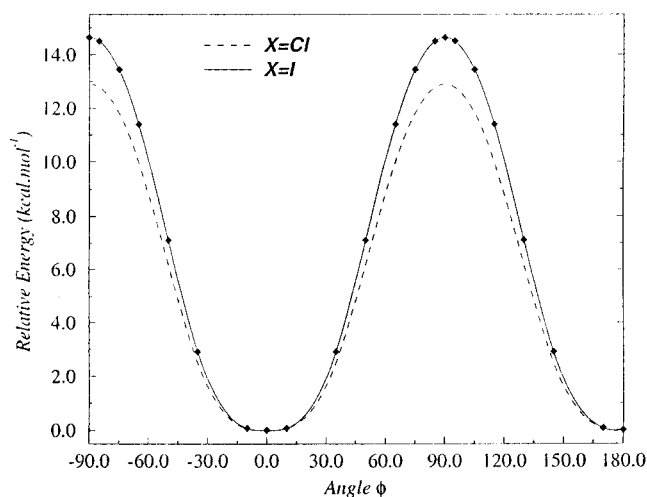
Figure 4. Potential energy surface $V(\phi)$ for H1/H2 exchange in OsH$_3$X-(PH$_3$)$_2$ (X = Cl, I).

be valid only if (i) there is no softer vibrational mode in the ground state which could make the molecule distort first in another direction and (ii) the movement of the two exchanging hydrogens is correlated. The out-of-plane bending of the hydrides has been calculated (RHF) to be the mode with the lowest frequency (456 cm^{-1}). The correlated motion of the two hydrogens is also calculated to be preferred to a motion of only one H. A two-dimensional map of the potential energy surface for out-of-plane motion of each hydride shows that the easiest motion out of the reference Π_0 plane is obtained when the two H's (rather than one) are displaced by equal angles.
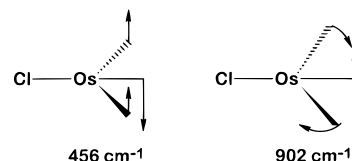
Even within the framework of correlated motion of H1 and H2, it is too time-consuming to calculate the potential energy, $V(\phi)$, by optimizing all structural parameters for every value of ϕ. It was thus necessary to calculate a simplified path with selected parameters frozen. In addition to freezing the P$-$H bond length and the H$-$P$-$Os angle, the Os$-$P distance was kept constant at 2.315 Å, a value intermediate between those in the ground state and in the transition state. All other variables were optimized. Under these conditions, a difference of energy of 12.9 kcal$\cdot$mol^{-1} is calculated between ground state ($\phi = 0°$) and transition state ($\phi = 90°$), which is very close to the value obtained in the absence of any constraint. In addition, the structures of the two extrema are very close to those obtained by full optimization. These results validate the chosen approximations.

The relative motion of the H centers is illustrated by the optimized values r_{eq}, θ_{eq}, and z_{eq} of the variables r, θ, and z as a function of ϕ (Table 2). The H1$-$H2 internuclear distance, r, is the most sensitive variable during the exchange and reaches its shortest value at the transition structure. At the same time, z, the distance between Os and the middle of the H1$\cdots$H2 unit, increases slightly. Any libration of the H1$-$H2 rotor is negligible, since θ_{eq} remains close to 90°. It means that the exchange of H1 and H2 occurs essentially in a plane perpendicular to the direction of the z vector.

The shape of the barrier is shown in Figure 4. The barrier for exchange was also calculated at a higher level of calculations (MP4SDQ, QCISD, QCISD(T), CCSD, and CCSD(T)). While the MP2 value was calculated to be 12.9 kcal$\cdot$mol^{-1}, the higher methods uniformly give a value of 14.3 ± 0.3 kcal$\cdot$mol^{-1}. The

influence of the nature of the phosphine was examined by calculating the ground state and the transition state structures of $OsH_3Cl(PMe_3)_2$ with the geometry of $OsH_3Cl(PH_3)_2$. The calculated activation energy decreases to 9.8 kcal·mol^{-1} at the MP2 level for the PMe_3 analog.

Influence of the Halide on the Energy Barrier for H1···H2 Exchange. Calculations were carried out for $OsH_3I(PH_3)_2$ following a similar procedure, leading to results which are similar to those obtained for Cl. The energy barrier (Figure 4) is calculated to be 14.6 kcal·mol^{-1} (MP2) and rises to 15.7 ± 0.2 kcal·mol^{-1} at higher levels of calculations (*vide supra*). Therefore, at all levels of calculation, the activation energy is higher for I than for Cl, which parallels the experimental values ($\Delta G^{\ddagger} = 8$ and 8.8 kcal·mol^{-1} for Cl and I, respectively).

Exchange Coupling in $(P^iPr_3)_2Os(H)_3ClL'$ ($L' = PEt_3$, CO, MeCN, NH_3, Acetone, THF-d_8, and Methanol). Ligands other than H_2[17] were added to $L_2Os(H)_3X$ for several reasons. First, since these complexes have only one X ligand, they are expected to be more Lewis acidic[19] than $L_2Os(H)_2X_2$, which binds N-based heterocycles.[26] This reactivity was probed for ligands with an array of donor ability, including PEt_3, CO, acetonitrile, acetone, methanol, THF, CD_2Cl_2, toluene, and methylcyclohexane. Second, the observation of exchange coupling in the adduct $L_2Os(H)_3X(H_2)$[17] inspired us to investigate the coupling in other adducts of $L_2Os(H)_3X$. As previously mentioned, most exchange coupling examples involve an MH_3 array with a molecular plane of symmetry through the central MH bond, so that only one coupling constant can be observed. In adduct $L_2Os(H)_3XL'$, this limitation is removed. Third, the observed temperature dependence in "solvents" (*vide infra*) might be better understood by using molecules with varying coordination ability.
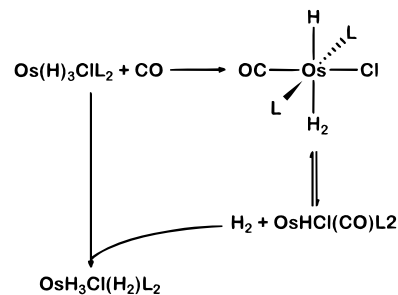
Formation of $(P^iPr_3)_2Os(H)_3ClL'$. General Features. These seven-coordinate complexes are synthesized in time of mixing by adding L' to a solution of **1**. In some cases, special care was taken to avoid coordination of additional equivalents of L', as discussed below. These seven-coordinate complexes are assigned a pentagonal bipyramidal geometry, with L' *cis* to chloride (**IV**, where P^iPr_3 ligands lie above and below this pentagonal plane). This geometry is the most favorable

IV
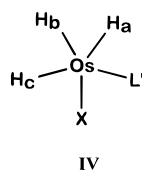
thermodynamically because it (1) minimizes steric interactions by putting bulky phosphines in *trans* positions and (2) avoids placing hydride ligands (the strongest σ-donors) in *trans* or pseudo-*trans* positions, and kinetically because it (3) places the incoming ligand in the position predicted by the LUMO of the unsaturated trihydride complex **I**, Figure 2. This molecular geometry is also calculated to be a global minimum for the model complexes $(PH_3)_3Os(H)_3Cl$ ($L' = PH_3$) (*vide infra*) and $(PH_3)_2Os(H)_3Cl(H_2)$ ($L' = H_2$).[17] In all cases (except $L' = CO$, *vide infra*), T_{1min} measurements of the hydrides in **IV** indicate no significant H–H bonding, consistent with the seven-coordinate geometry.

$L' = PEt_3$. Structure "Proof" of the Seven-Coordinate Molecules. When **1** is dissolved in CD_2Cl_2 and 0.9 equiv of PEt_3 is added, the binding of the phosphine is complete within less than 10 min. The $^{31}P\{^1H\}$ NMR spectrum shows a doublet ($J_{PP} = 16$ Hz, 2P) at 18.7 ppm and a triplet ($J_{PP} = 16$ Hz, 1P)

(26) Esteruelas, M. A.; Lahoz, F. J.; Oro, L. A.; Oñate, E.; Ruiz, N. *Inorg. Chem.* **1994**, *33*, 787.

Scheme 1

at -23.7 ppm at 20 °C. The P/P coupling constant of 16 Hz is consistent with PEt_3 binding in the equatorial plane of a pentagonal bipyramid, as in **IV**. Measurement of T_1 indicates that the hydrides remain classical in the seven-coordinate complex. In the hydride region of the ^1H NMR, two signals are observed throughout the temperature range from 0 to -100 °C, in the ratio 2:1; the signals coalesce at approximately 35 °C. Since phosphine dissociation is negligible in this temperature range (P/P coupling is observed at 25 °C), the hydride coalescence is attributed to intramolecular motions of the hydride ligands in the intact, seven-coordinate molecule.

The hydride signal of intensity two remains broad at the lowest available temperature and appears at -14.8 ppm, while the signal of intensity 1 at -6.21 ppm sharpens to a doublet of triplets ($J_{HP} = 71.1$ Hz, $J_{HP} = 20.5$ Hz) at -80 °C. Due to the large H/P coupling constant of the hydride at -6.2 to the P of PEt_3, we assign it a position transoid to L', as H_c in **IV**. The T_1 values at -80 °C show that the two fast-exchanging hydrides also have the faster relaxation ($T_1 = 81$ ms) compared to the other hydride ($T_1 = 132$ ms). This probably indicates that the distance $H_a···H_b < H_b···H_c$ in **IV**. This conclusion is in agreement with the calculation on the model complex $(PH_3)_3$-$Os(H)_3Cl$ (*vide infra*), which finds an $H_a···H_b$ separation of 1.59 Å and an $H_b···H_c$ separation of 1.67 Å.

No hydride–hydride coupling is observed at any temperature. Low-temperature spectra of $L_2OsH_xD_{3-x}Cl(PEt_3)$ are essentially the same as those of the all-protio complex in the hydride region, discounting the possibility of deceptively simple spectra due to very large exchange coupling. While the choice $L' = PEt_3$ was useful for initial exploration of ligand binding to $L_2Os(H)_3Cl$, giving information by virtue of P–P and H–P couplings, we see no evidence for exchange coupling in $L_2Os(H)_3Cl(PEt_3)$. According to the theory and results of Zilm and Heinekey,[3] exchange coupling is diminished when ligand L' is more electron-donating (i.e., when $\nu(M-H)$ increases). Thus, we felt that our chances of finding exchange coupling may be enhanced by choice of L' which does not make the metal center electron-rich due to σ donation and, therefore, tried the π-accepting ligand CO.

$L' = CO$. The addition of less than 1 equiv of CO to **1** in toluene-d_8 gives the known complex $L_2OsH(H_2)Cl(CO)$[27] (with H *trans* to H_2) as one product. This complex then transfers H_2 to remaining **1**, yielding $L_2Os(H)_3Cl(H_2)$ and $L_2OsHCl(CO)$ as additional products (see Scheme 1). Even when the reaction is performed carefully at -90 °C, no intermediates (such as L_2-$OsH(H_2)Cl(CO)$, with H *cis* to H_2, or $L_2Os(H)_3Cl(CO)$) are observed. This is typical reactivity for CO with an unsaturated polyhydride complex: CO does not simply add but effects reductive elimination of H_2.

In this case, we have exactly the opposite problem from $L' = PEt_3$—too little donation from L'. We have decreased electron

(27) Andriollo, A.; Esteruelas, M. A.; Meyer, U.; Oro, L. A.; Sanchez-Delgado, R. A.; Sola, E.; Valero, C.; Werner, H. *J. Am. Chem. Soc.* **1989**, *111*, 7431.
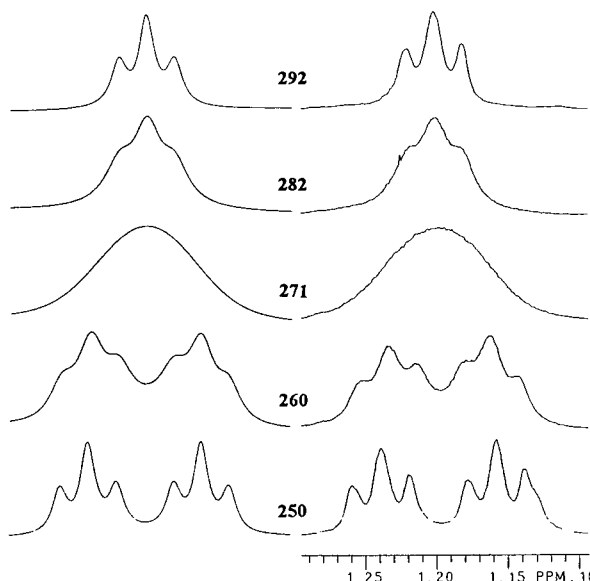
Figure 5. Experimental (right) and simulated ^{1}H NMR spectra for the ^{i}Pr methyl signals of $(P^iPr_3)_2OsH_3Cl(MeCN)$. The methine signal has been decoupled. Temperatures in kelvin.

Figure 6. Variable-temperature (°C) ^{1}H NMR spectra (hydride region) of $L_2Os(H)_3Cl(NH_3)$ in toluene-d_8.

density on the hydrides to the point where an H−H bond is formed. At this point, we decided to add simple σ-donating ligands which bind more weakly than PEt$_3$.

Lewis Bases of High Binding Ability. General Comments on Kinetics of L′ Dissociation. The ligands NH$_3$ and MeCN bind quite tightly, so that, at all available temperatures in toluene-d_8, the hydride signal observed is that for $L_2Os(H)_3ClL'$. The hydrides show a single (coalesced) signal at temperatures above 10 °C, due to fast intramolecular hydride site exchange.

Kinetic data regarding the rates of L′ loss from these seven-coordinate species are available for $L_2Os(H)_3Cl(NH_3)$ and L_2-$Os(H)_3Cl(MeCN)$ from the i-Pr methyl region of the variable-temperature ^{1}H NMR spectrum. Binding of L′ destroys the vertical mirror plane of symmetry which was present in L_2Os-$(H)_3Cl$. Consequently, the methyl groups of the P^{i}Pr$_3$ ligands are diastereotopic, and two apparent quartets are observed. At increased temperature, L′ dissociation becomes rapid on the NMR time scale, and the two methyl signals coalesce (Figure 5). The rate of ligand loss is higher for MeCN than for NH$_3$. By simulating these spectra (using DNMR5), rate constants for L′ dissociation are determined (see Supporting Information).[28]

L′ = MeCN. The compound $L_2OsH_3Cl(MeCN)$ can easily be studied spectroscopically, since subsequent reactions (which generate ionic species, *vide infra*) do not occur appreciably in the nonpolar solvent, toluene-d_8. At room temperature, a single resonance is seen in $^{31}P\{^1H\}$ NMR spectra for the seven-coordinate complex $L_2Os(H)_3Cl(MeCN)$. In the alkyl region, one i-Pr methyl signal (apparent quartet) appears at room temperature and decoalesces (∼0 °C) to two apparent quartets, at δ 1.31 and 1.18 ppm. The activation parameters for MeCN dissociation from $L_2Os(H)_3Cl(MeCN)$ have been determined as discussed above: $\Delta H^{\ddagger} = 17.6(3)$ kcal/mol and $\Delta S^{\ddagger} = 14.7(9)$ cal/(mol K).

In the hydride region, a room-temperature triplet (−12.69 ppm, $J = 13.1$ Hz) decoalesces into two very broad resonances at −10.1 (1H) and −13.5 (2H) ppm. The T_{1min} for the averaged signal (82 ms) occurs at −48 °C and is slightly longer than that observed for **1** (72 ms). At −90 °C, the signal at −10.1 ppm has a shorter T_1 value (230 ms) than that at −13.5 ppm (300 ms). The coalescence of the two hydride signals has been simulated, yielding activation parameters of $\Delta H^{\ddagger} = 6.08(1)$ kcal/
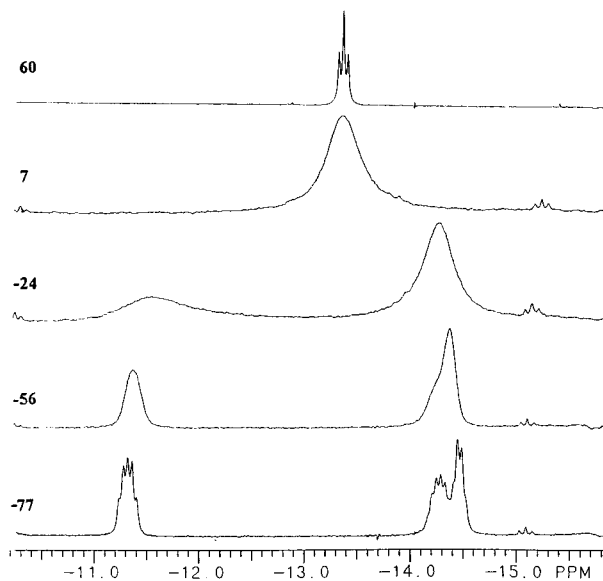
mol and $\Delta S^{\ddagger} = -11(1)$ cal/(mol K). This process is very clearly different than MeCN dissociation, since it is a nondissociative process ($\Delta S^{\ddagger} < 0$) with much lower $\Delta H^{\ddagger}$ than that measured for MeCN dissociation (see above). These activation parameters, therefore, must correspond to intramolecular hydride site exchange. Since three hydride resonances are expected in this seven-coordinate complex (see **IV**), it is unclear whether these activation parameters correspond to H$_a$/H$_b$ exchange or H$_b$/H$_c$ exchange. By analogy to structural assignments made in the PEt$_3$-ligated complex, H$_c$ in the MeCN adduct is the resonance at −10.1 ppm. It follows that the activation parameters measured for the coalescence of the 2:1 spectrum may be for exchange between H$_b$ and H$_c$. This $\Delta H^{\ddagger}$ is within the range in which exchange coupling is typically observed.

Virtually the same variable-temperature hydride NMR is observed using a partially deuterated sample, $L_2OsH_xD_{3-x}$-$Cl(MeCN)$. Once again, the deuterated complex was investigated in order to probe the possibility of very large exchange coupling leading to deceptively simple NMR patterns. Even though MeCN dissociates more readily than NH$_3$ (and, therefore, seems to be a weaker donating ligand), no exchange coupling is observed in the *partly* decoalesced ^{1}H NMR spectrum of L_2-$Os(H)_3Cl(MeCN)$. For some reason, the hydride ligands exchange sites much more easily than they do in the NH$_3$ adduct complex (*vide infra*), precluding complete low-temperature decoalescence of the hydride signals. Thus, neither the presence nor the absence of exchange coupling in this complex is definitively established for the remaining two fluxional hydrides.

L′ = NH$_3$. Ammonia coordinates quite strongly to **1**, with the seven-coordinate complex $L_2Os(H)_3Cl(NH_3)$ being the only observable species at room temperature in toluene-d_8. A broad ^{1}H NMR signal for coordinated NH$_3$ appears at 2.25 ppm. Kinetics of NH$_3$ dissociation from $L_2Os(H)_3Cl(NH_3)$ have been determined by coalescence of the i-Pr methyl signals, as discussed above. The spectra and simulations for this case are similar in appearance to those for MeCN loss (Figure 5). Eyring analysis gives the activation parameters: $\Delta H^{\ddagger} = 20.7(3)$ kcal/mol and $\Delta S^{\ddagger} = 16(1)$ cal/(mol K) for NH$_3$ loss. These values set the limits $\Delta H° \leq -20.7(3)$ kcal/mol and $\Delta S° = \leq -16(1)$ cal/(mol K) for NH$_3$ coordination.

Variable-temperature hydride NMR spectra in toluene-d_8 are shown in Figure 6. After decoalescence at about −20 °C, three hydride signals are observed. At about −70 °C, H/H coupling is resolved: 26 and 13 Hz in toluene-d_8 and 150 and 0 Hz in

---

(28) The methine signals were decoupled during acquisition to simplify the spectra and the simulation.

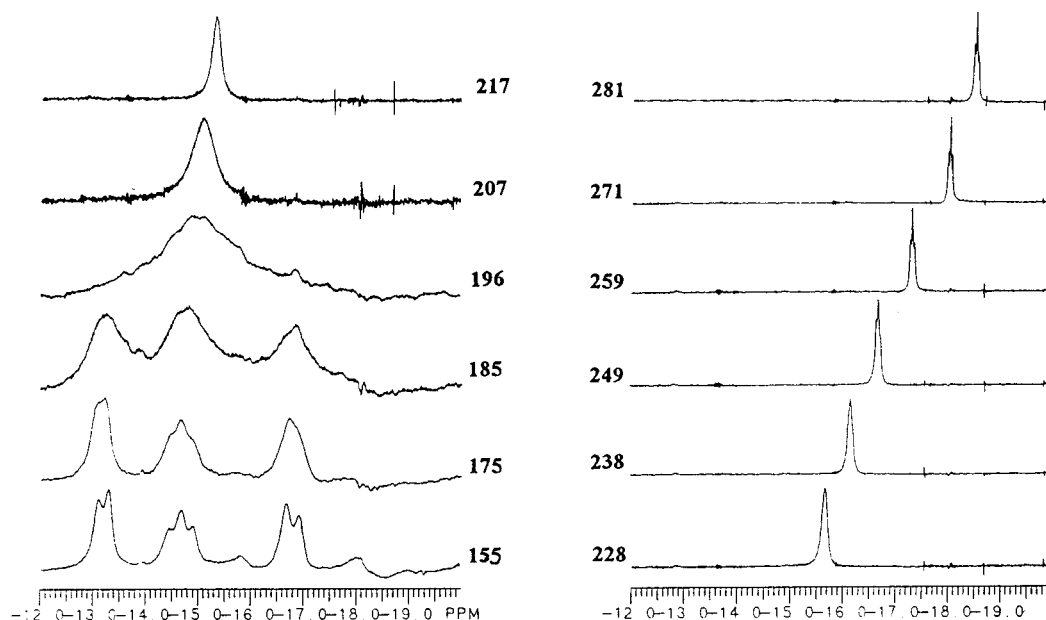**Figure 7.** Variable-temperature (K) ^{1}H NMR spectra of the hydride signals of $L_2Os(H)_3Cl$ in equilibrium with $L_2OsH_3Cl(MeOH)$ in CD_2Cl_2.

CD_2Cl_2. This remarkable solvent dependence of J is an indication of the amazing sensitivity of exchange coupling to slight molecular differences. The larger coupling in CD_2Cl_2 probably indicates that NH_3 is acting as a poorer donor in this solvent than in toluene-d_8. The reduced donicity may be due to hydrogen bond formation between Cl of the solvent and protons of the NH_3 ligand. We present evidence below for chloride ion hydrogen bonding to protons of coordinated NH_3 in the solid state structure of $[Os(H)_3(NH_3)_2(P^iPr_3)_2]Cl$. Hydrogen bonding has been invoked to explain the change in NH and CN stretching frequencies in $(NH_3)_5Ru(RCN)^{2+}$ with change in counterion.[29] Complexes in this series with good hydrogen bond-acceptor anions have higher ν_{CN} values.

Thus, in $L_2Os(H)_3Cl(NH_3)$, we have not only seen H/H couplings but are able to observe subtle effects of changing solvent. While 26 and 13 Hz might be argued to be too small to be exchange couplings, 150 Hz is not generally considered to be within the range of normal magnetic H/H couplings. In addition, such a tremendous solvent effect has not before been observed for "normal" couplings, so it seems likely that we have exchange coupling in this complex. We have thus probed even weaker σ-donating ligands in attempts to increase J_{ex}.

Lewis Bases of Intermediate Binding Ability. General Comments on Thermodynamics of L′ Binding. The ligand-binding thermodynamics and spectroscopic characterization of each of the complexes are discussed individually, but this section presents some information common to several L′ ligands. In the presence of THF-d_8, acetone, or CH_3OH, similar NMR behavior is observed. At room temperature, the observed hydride NMR signal is simply that of $L_2Os(H)_3Cl$. As the temperature is lowered, the hydride chemical shift moves, until it eventually becomes constant at the chemical shift of L_2Os-$(H)_3ClL′$ (e.g., Figure 7) For comparison, the chemical shift of **1** in toluene-d_8, methylcyclohexane-d_{14}, or CD_2Cl_2 in the absence of added L′ is temperature-invariant, within the precision of the measurement. We assume in the following analysis that the chemical shift of the seven-coordinate $L_2OsH_3ClL′$ species is also temperature-independent. At intermediate temperatures, the chemical shift is an indicator of the position of
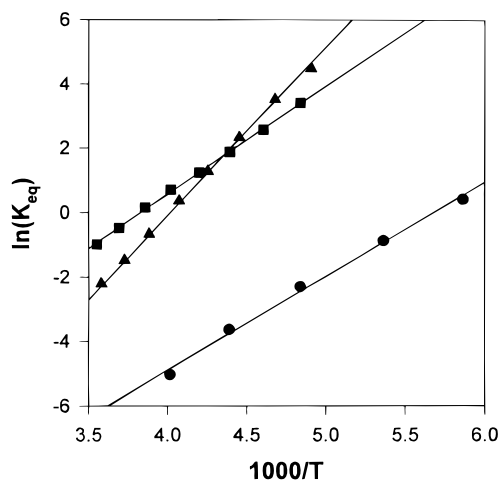
(29) Chatt, J.; Leigh, G. J.; Than Karajan, N. *J. Chem. Soc. A* **1971**, 3168.

(30) Smith, K.-T.; Tilset, M.; Kuhlman, R.; Caulton, K G. *J. Am. Chem. Soc.* **1995**, *117*, 9473.

Figure 8. Van't Hoff plots for equilibrium binding of THF-d_8 (●), acetone (■), and methanol (▲) to $L_2Os(H)_3Cl$.

the equilibrium L′ binding, according to eqs 6 and 7, in which

$$[ML′] = M_o\left[\frac{\delta - \delta_{av}}{\delta - \delta′}\right] \qquad (6)$$

$$K_{eq} = \frac{[ML′]}{[M](L_o′ - [ML′])} \qquad (7)$$

M represents the 16-electron complex, L′ is the added ligand, $M_o = [M] + [ML′]$, $L_o′ = [L′] + [ML′]$, δ is the chemical shift of 16-electron complex, $\delta′$ is the chemical shift of 18-electron complex, and δ_{av} is the observed chemical shift. Thus, K_{eq} is determined as a function of T, and $\Delta H°$ and $\Delta S°$ are obtained from $\ln(K)$ vs $1/T$ plots (Supporting Information and Figure 8). The order of solvent ligand binding in terms of $\Delta H°$ is acetone > MeOH > THF-d_8.

L′ = Acetone. In CD_2Cl_2, acetone binds to **1** in a reversible equilibrium. As the temperature decreases, the hydride signal shifts upfield before decoalescing at about -100 °C. By plotting $\ln(K_{eq})$ vs $1/T$, we obtain $\Delta H° = -10.4(1)$ kcal/mol and $\Delta S° = -41.8(5)$ cal/(mol K) for acetone binding. The decoalesced hydride region of the spectrum is difficult to interpret, since the signals are close together and quite broad. It is consistent with an ABC pattern having J_{HH} values of about 60 and 30 Hz and chemical shifts of -12.9, -13.7, and -14.0 ppm. The T_{1min}

for the coalesced hydride signal is less than 65.2 ms and is measured at about −77 °C (equilibrium shifted almost exclusively to the seven-coordinate complex). This faster (than in **1**) relaxation indicates that at least one H−H separation is shorter than 1.59 Å (the distance in **1**). The shorter distance may simply be a consequence of adding a fairly bulky ligand (note that $\Delta S°$ is −41.8 cal/(mol K)) and most likely does not indicate significant H−H bonding. The T_{1min} value is similar to that observed for the trihydride $L_2OsH_3(MeCN)_2^{+}$.[30]

L′ = Methanol. When 13 equiv of CH_3OD is added to a THF-d_8/toluene-d_8 (9:1) solution of **1**, evidence for the complex $L_2Os(H)_3Cl(CH_3OD)$ can be seen in ${}^1H$ NMR. At room temperature, a broad signal is observed at −18.50 ppm, which shifts farther downfield at lower temperatures and then finally decoalesces into three resonances of equal intensity at −12.47 (d, J = 70 Hz), −14.88 (d, J = 70 Hz), and −16.97 ppm (br s). After several hours at 20 °C, deuterium from CH_3OD is incorporated into the metal hydride positions.

The behavior of $L_2Os(H)_3Cl$ with MeOH in CD_2Cl_2 is different than in THF. Once again, one sees evidence for equilibrium binding of MeOH (Figure 7), which binds with $\Delta H°$ = −6.66(8) kcal/mol and $\Delta S°$ = −25.5(3) cal/(mol K). The T_{1min} value measured at −66 °C is 70.4 ms. At −110 °C, once again three resonances are seen, but this time there are two values of J_{HH}: δ −13.22 (d, J_{HH} = 55 Hz), −14.71 (broad apparent triplet, outer line separation of 133 Hz), and −16.80 (d, J_{HH} = 73 Hz). This change in magnitude of exchange coupling, which is especially dramatic for the −16.8 ppm hydride, is attributed to variable hydrogen bonding in THF/toluene *vs* in that CD_2Cl_2.

In toluene-d_8 in the presence of 7 equiv of MeOH, again decoalescence can be seen to three resonances, but they are too broad at available temperatures for coupling to be observed. The line widths of the signals are 120, 150, and 110 Hz at −98 °C for δ −13.06, −14.70, and −16.50, respectively.

L′ = THF-d_8. A solution of **1** in THF-d_8/toluene-d_8 (7:3) shows evidence for THF binding at lower temperatures. As the temperature decreases, the hydride signal shifts upfield before decoalescing at about −100 °C. In the hydride region at −113 °C, three resonances are seen at δ −12.1 (d, J = 320 Hz), −14.9 (d, J = 320 Hz), and −17.84 (br s). We obtain $\Delta H°$ = −5.8(2) kcal/mol and $\Delta S°$ = −33(1) cal/(mol K) for THF binding. No T_{1min} value can be obtained for this seven-coordinate complex, since there is significant population of THF-free $L_2Os(H)_3Cl$ in fast exchange around the temperature of T_{1min}. This L′ is the weakest donor (least negative $\Delta H°$) and has the largest exchange coupling of the $L_2Os(H)_3ClL′$ series (excluding L′ = H_2).[17]

Reactions Subsequent to 1:1 Adduct Formation. Formation of $L_2OsH_3L′_2^{+}Cl^{-}$. In CD_2Cl_2, when MeCN or NH_3 is added to **1**, the ligand subsequently displaces Cl^{-} to the outer coordination sphere (eq 8). This reaction is quite slow or even

$$L_2Os(H)_3XL′ + L′ \rightleftharpoons [L_2OsH_3L′_2^{+}] + X^{-} \quad (8)$$
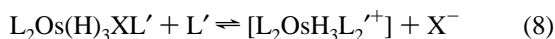
unobserved in toluene-d_8 (depending on the L′:Os ratio employed) but occurs on the time scale of several hours in CD_2Cl_2. The second L′ presumably takes the position of the departed chloride ligand, maintaining the pentagonal-bipyramidal geometry.

(a) L′ = NH_3. If a toluene solution of **1** is allowed to stand under an atmosphere of NH_3 overnight, NH_3 displaces Cl^{-} to the outer coordination sphere, and colorless crystals of $[L_2OsH_3(NH_3)_2]^{+}Cl^{-}$ precipitate. The crystals are readily soluble in CD_2Cl_2, but some of the NH_3 dissociates in this solvent in the absence of excess NH_3, so signals for both $[L_2OsH_3(NH_3)_2]^{+}$ and $L_2OsH_3Cl(NH_3)$ appear in the spectrum.
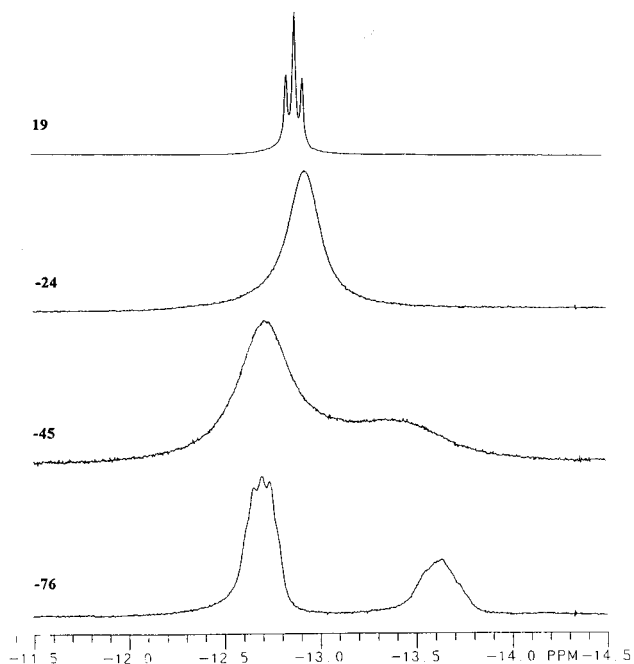
Figure 9. Variable-temperature (°C) ${}^1H$ NMR spectra (hydride region) of $L_2Os(H)_3(NH_3)_2^{+}$ in CD_2Cl_2.

Under excess NH_3 in CD_2Cl_2, $[L_2OsH_3(NH_3)_2]^{+}$ forms quantitatively.[31] Unlike the analogous bis-MeCN complex,[30] the hydride signal in this complex decoalesces at about −50 °C (Figure 9). At −70 °C, two hydride signals are clearly resolved, at δ −12.7 (2H) and −13.6 (1H). The signal at δ −12.7 appears as a doublet of triplets with J_{HH} = 25 Hz and J_{HP} = 13 Hz (J_{HP} = 12.3 Hz in the averaged resonance at +19 °C). Neither of the signals has particularly fast relaxation: T_{1min} for the three resonances is 81.0 ms, taken from the weighted average of the T_1's at −58 °C. The unit intensity hydride relaxes faster than the hydrides of integration two throughout the temperature range from −48 to −78 °C. Both the absolute and relative magnitudes of these T_1 values are consistent with a pentagonal-bipyramidal trihydride structure. The alternate formulation, $L_2Os(NH_3)_2H$-$(H_2)^{+}$, would almost certainly have a shorter T_{1min} (<40 ms/300 MHz) and with absolute certainty would have the signal of intensity 2 relaxing faster than that of integration 1. The structure was determined for L′ = NH_3 by X-ray diffraction.

X-ray Structure of $[L_2OsH_3(NH_3)_2]Cl$. The structure of the bis-NH_3 adduct was determined by X-ray diffraction and is depicted by an ORTEP diagram in Figure 10. Bond lengths and distances are included in Table 3. Neither the hydride ligands nor the hydrogens on the ammonia ligands were located in the Fourier map. Attempts at placing the hydrides using the program XHYDEX gave ambiguous results.

The phosphines are slightly distorted from *trans* positions, with P−Os−P angle of 167.24(7)°. The angle less than 180° is most likely due to steric interactions with the NH_3 ligands, which (although not especially large ligands) are bulkier than hydrides. The NH_3 ligands occupy adjacent positions, with an N−Os−N angle of 81.5(2)°. This angle is less than 90°, indicating the likelihood of more than four ligands in the equatorial plane; therefore, this angle supports the pentagonal bipyramidal proposal with an $Os(H)_3$ and not an $OsH(H_2)$ substructure. Accordingly, a molecular plane of symmetry should pass through P−Os−P and one hydride, with one hydride and one NH_3 on each side of the plane. As expected, the P−Os−P plane is perpendicular to N−Os−N (intersection angle is 90.5°). However, there is some slight deviation from the

---

(31) After several days, further reaction leads to precipitation of a white solid, and the solution turns green.
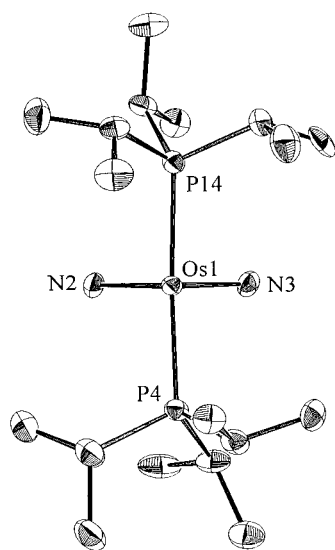
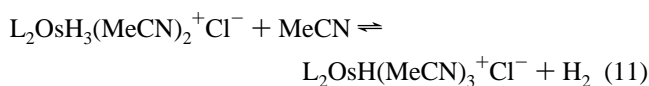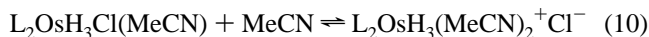**Figure 10.** ORTEP drawing of nonhydrogen atoms of $(P^iPr_3)_2Os(H)_3$-$(NH_3)_2^+$.

Table 3. Selected Bond Distances (Å) and Angles (deg) in $L_2OsH_3(NH_3)_2^+Cl^-$

Os1−P4	2.328(2)	Os1−N2	2.232(6)
Os1−P14	2.324(2)	Os1−N3	2.231(6)
P4−Os1−P14	167.24(7)	P14−Os1−N2	95.8(2)
P4−Os1−N2	95.5(2)	P14−Os1−N3	94.4(2)
P4−Os1−N3	93.1(2)	N2−Os1−N3	81.5(2)

expected C_{2v} symmetry; both phosphines are slightly closer to N3 than to N2: P4/N2 = 3.38 Å, P4−N3 = 3.31 Å, P14−N2 = 3.38 Å, P14−N3 = 3.34 Å. This asymmetry in the molecule indicates some slight distortion from a rigorous pentagonal-bipyramidal geometry, perhaps due to crystal packing effects or some ruffling (noncoplanarity) of the three hydride ligands.

There is some evidence for weak hydrogen bonding in this structure. It was mentioned above that hydrogen bonding to CD_2Cl_2 could explain the remarkable solvent dependence of J in $L_2OsH_3Cl(NH_3)$, so it was reasonable to anticipate some H···Cl⁻ hydrogen bonding in this complex. The shortest H···Cl distance (ammonia hydrogens in fixed calculated positions) is 2.49 Å. While this distance is not remarkably short, it is shorter than those hydrogen-bonded distances observed by neutron diffraction in $(P^iPr_3)_2IrCl_2H(H_2)$ (2.64−2.65 Å).[32] The chloride is not hydrogen-bonding to a hydride on osmium, since the shortest Cl−Os distance is 4.660(3).

(b) L′ = MeCN. Acetonitrile adds rapidly and reversibly to **1** to first form the seven-coordinate complex (eq 9). In CD_2Cl_2, a second and then a third equivalent of MeCN slowly add, consecutively displacing Cl⁻ (eq 10) and H_2 (eq 11). The

$$L_2OsH_3Cl + MeCN \rightleftharpoons L_2OsH_3Cl(MeCN) \qquad (9)$$

$$L_2OsH_3Cl(MeCN) + MeCN \rightleftharpoons L_2OsH_3(MeCN)_2^+Cl^- \quad (10)$$

$$L_2OsH_3(MeCN)_2^+Cl^- + MeCN \rightleftharpoons$$
$$L_2OsH(MeCN)_3^+Cl^- + H_2 \quad (11)$$

reactions of eqs 10 and 11 take place on the time scale of days at room temperature. Shown in Figure 11 is the time evolution of the concentration of these three species upon addition of 24 equiv of MeCN. The dashed lines on the plot are simulated
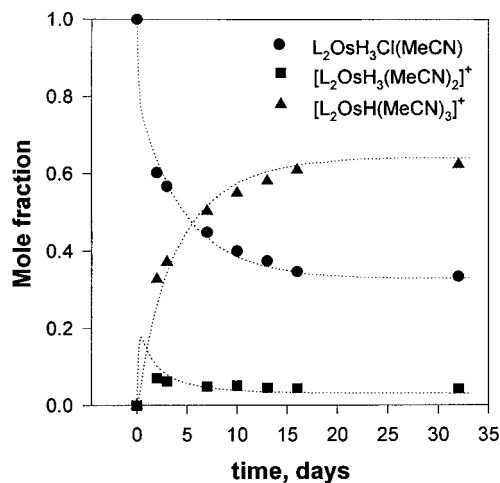
(32) Albinati, A.; Bakhmutov, V. I.; Caulton, K. G.; Clot, E.; Eckert, J.; Eisenstein, O.; Gusev, D. G.; Grushin, V. V.; Hauger, B. E.; Klooster, W. T.; Koetzle, T. F.; McMullan, R. K.; O'Loughlin, T. J.; Pélissier, M.; Ricci, J. S.; Sigalas, M. P.; Vymenits, A. B. *J. Am. Chem. Soc.* **1993**, *115*, 7300.

Figure 11. Time evolution of the reaction of $L_2Os(H)_3Cl$ with MeCN in CD_2Cl_2. Calculated profiles (dotted lines) use rate constants given in the text.

concentration profiles using the program GEAR[33] and the following conditions: $[L_2Os(H)_3Cl(MeCN)]_o = 0.036$ M, $[MeCN]_o = 0.874$ M, $k_{10} = 1.30$, $k_{-10} = 468$, $k_{11} = 1.15$, $k_{-11} = 1.95$ (all M⁻¹ d⁻¹), where the rate constants refer to the forward and reverse directions of the reactions in eqs 10 and 11. These rate constants are only approximate because they do not take into account any evolution of H_2 from the solution. The forward rate constants of eqs 10 and 11 yield $\Delta G^\ddagger$ (25 °C) of 24 kcal/mol. These bis- and tris-acetonitrile cationic complexes have recently been synthesized (with counteranion BF_4^-) by protonation of L_2OsH_6 in MeCN.[30] The rate of formation of $L_2OsH(MeCN)_3^+$ from $L_2OsH_3(MeCN)_2^+$ here is consistent with this earlier report.

(c) Dehydrogenation of Methanol. No hydride signal for **1** is observed after several minutes at room temperature in *pure* CD_3OD, presumably due to exchange of hydrides with OD. If **1** is dissolved in neat CH_3OH, $L_2OsH(H_2)(CO)Cl$ crystallizes out of the solution as colorless crystals after about 1 day at room temperature. When the crystals are isolated, some H_2 is lost so that NMR and IR spectra show mixtures of L_2OsH-$(H_2)(CO)Cl$ and $L_2OsH(CO)Cl$. Such dehydrogenation of MeOH by metal species has been observed at high temperatures in the synthesis of $L_2MH(CO)Cl$ (M = Ru, Os).[34]

Theoretical Studies of the 16- and the 18-Electron Species. The influence of an additional ligand or a solvent has been modeled by calculations on the seven-coordinate species OsH_3-$Cl(PH_3)_3$. The additional ligand might coordinate in the plane Π_0, which contains the hydride either *cis* to the halide or pseudo-trans to it (i.e., *cis* to two hydrides). Preliminary calculations showed that the coordination of the added ligand is favored *cis* to the halide; this is also in agreement with the shape of the LUMO of OsH_3XL_2 (Figure 2), which is mostly developed *cis* to the halide. It also agrees with the structure of $Os(H_2)H_3$-XL_2, where a dihydrogen ligand is *cis* to X.[17]

The optimization of the structure at the MP2 level (Figure 12, Table 1) gives a result which is best viewed as a pentagonal bipyramid with angles in the equatorial plane ranging from 63° to 84°. The most important bond length change with respect to the unsaturated complex is the significant lengthening of the Os-Cl bond (2.487 *vs* 2.374 Å), which is due to the loss of the Os−Cl π-bond in the 18-electron species.

(33) (a) Stabler, R. N.; Chesick, J. *Int. J. Kinet.* **1978**, *10*, 461. (b) McKinney, R. J.; Weigert, F. J., Quantum Chemistry Program Exchange, No. QCMP022.

(34) (a) Moers, F. G.; Langhout, J. P. *Rec. Trav. Chim. Pays-Bas* **1972**, *91*, 591. (b) Gill, D. F.; Shaw, B. L. *Inorg. Chim. Acta* **1979**, *32*, 19.
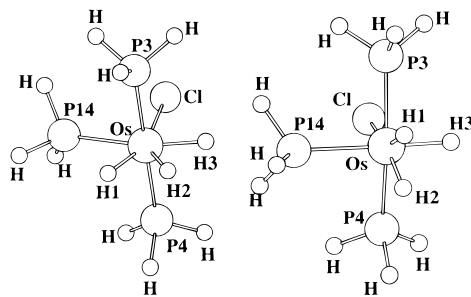
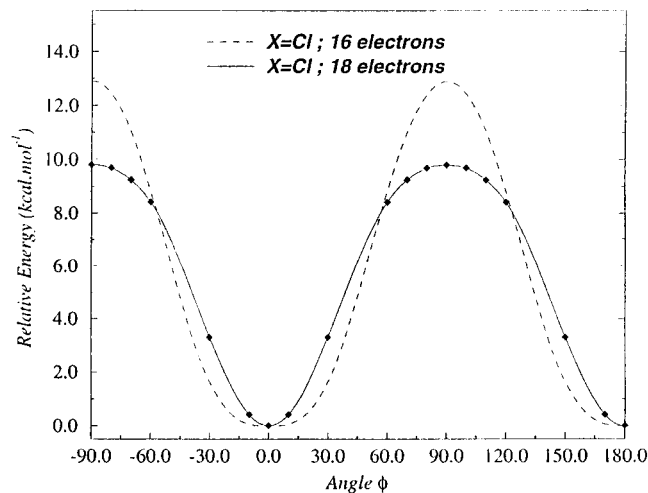**Figure 12.** Optimized structures for the ground state and transition state for H1/H2 exchange in OsH₃Cl(PH₃)₃.

Figure 13. Potential energy surface $V(\phi)$ (kcal·mol^{-1}) for H1/H2 exchange in OsH₃Cl(PH₃)$_n$ (n = 2, 3).

Table 4. Temperature Dependence of J in L₂Os(H)₃X (X = Cl, Br, I, OCH(CF₃)₂ in Methylcyclohexane-d_{14}, Toluene-d_8, and CD₂Cl₂^a

Cl		Br		I		OCH(CF₃)₂					
T	J^b	T	J^b	T	J^b	T	J^b	T	J^c	T	J^d
−114	810	−119	512	−113	233	−87	40.5	−87	41.4	−112	53.7
−109	765	−114	494	−108	231	−77	39.9	−77	40.4	−106	53.3
−103	720	−108	464	−103	224	−66	39.4	−71	40.7	−101	53.4
−98	670	−103	437	−98	216					−95	52.8
−92	585	−98	412	−92	209					−90	51.3
		−92	376	−87	200					−83	50.7
		−87	352	−82	180					−77	48.8

^{a} Temperatures are in °C, and coupling constants are in hertz. ^{b} In methylcyclohexane-d_{14}. ^{c} In toluene-d_8. ^{d} In CD₂Cl₂.

calculation. The shape of the potential as a function of ϕ is shown in Figure 13, together with that of the 16-electron species. The most striking difference is the lowering of the activation energy in the 18-electron species, which is probably related to the intrinsically more fluxional behavior of a seven-coordinate complex. A widening of the barrier is also apparent and may also influence the calculated J.

"Abnormal" Temperature Dependence of Exchange Coupling in "Solvents". Originally, exchange couplings were measured in toluene-d_8, which, unfortunately, freezes (−95 °C) only slightly below the decoalescence temperature of the hydride signals. Thus, the temperature dependence of J could not be measured in this solvent. This problem was overcome by use of methylcyclohexane-d_{14}, which freezes at −126 °C. This solvent also has the unforeseen and unprecedented advantage of raising the decoalescence temperature of the hydride signals. The temperature dependence could now be observed over about a 20−30 °C temperature range.

Shown in Figure 14 are experimental and simulated variable-temperature spectra of **1** in methylcyclohexane-d_{14}. Since the signals were quite broad, simulations were necessary for accurate (±10 Hz) determination of J. Variable-temperature spectra for **2** and **3** (not shown) were analyzed in the same way.

Values of J *vs* T are given in Table 4 and Figure 15 for **1−4**. Amazingly, J is found to *decrease* with *increasing* temperature. This temperature dependence is opposite to every other reported exchange-coupled system. Furthermore, there is a distinct solvent dependence: J is larger in toluene than it is in methylcyclohexane. There are at least five possible explanations for the inverse temperature dependence: (1) J_m ("normal" magnetic coupling) and J_{ex} are of opposite sign, and $|J_m| > |J_{ex}|$ at all temperatures. (2) Measurements are made at the low-temperature region of the J *vs* T curve (*vide infra*), before it passes through zero. (3) J is influenced by equilibrium

Because of the lowered symmetry, exchanging H1 and H2 is not equivalent to exchanging H2 and H3. Preliminary calculations on the two transition states show that exchanging H1 and H2 is energetically easier than exchanging H2 and H3. A complete study was thus carried out on the exchange of H1 and H2 with the procedure used previously. The resulting structure for the transition state (Figure 12) is a trihydride with coplanar Os, H3, Cl, and the added phosphine P14. The exchanging hydrides and the axial phosphine (significantly bent) are approximately coplanar with Cl. The distance between the exchanging hydrides is significantly shorter in the TS (1.38 Å) than in the ground state (1.59 Å). However, the electronic effect (i.e., donor) of the chloride opposite to these two hydrides prevents a further decrease of the H1⋯H2 distance.

The activation energy is calculated to be 9.8 kcal·mol^{-1} at the MP2 level and 10.3 ± 0.2 kcal·mol^{-1} at higher levels of

Figure 14. Observed (left) and simulated variable-temperature (°C) hydride region ^{1}H NMR spectra of L₂Os(H)₃Cl in methylcyclohexane-d_{14}.
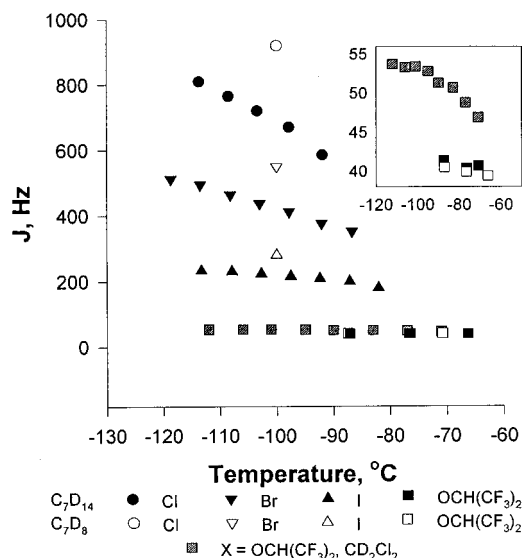
Figure 15. Temperature dependence of J in $L_2Os(H)_3X$. The inset shows data for $L_2Os(H)_3[OCH(CF_3)_2]$, to show more clearly the curvature and solvent dependence.

dimerization of the complex. (4) J is influenced by a fast, reversible, temperature-dependent solvent interaction. (5) J is affected by an agostic interaction from a phosphine alkyl group. The first explanation (canceling effect of J_m and J_{ex}) can be very simply ruled out by the magnitude of the coupling observed, which is much too large to be exceeded by magnetic coupling. For example, J_m in **1** would have to exceed 620 Hz, which is much larger than the accepted upper limit of 280 Hz, the value in H_2.

Early-on-the-Curve Explanation. It has been shown empirically that J_{ex} increases exponentially with temperature, and some theoretical basis for this has been described.[8] The value of J is summed over a Boltzmann distribution of rotational and vibrational levels, $J = \sum_n \chi_n J_n$, where χ_n indicates the fraction of the nth rovibrational state occupied in the complex at a given temperature, and J_n is the level splitting in that energy state. As the temperature increases, the population of higher energy rovibrational states also increases. Already, $J(T)$ is not a simple exponential, since rotational and vibrational levels are coupled and individual values of J_n do not increase monotonically. Moreover, calculations have shown that the *sign* of J_n varies with n (*vide infra*), and positive and negative contributions have a canceling effect in the summation of J_n. Nonetheless, simulations and experimental data for the most part show a roughly exponential dependence of J_{ex} on T.

The important point is that J_1 (coupling constant for the lowest rovibrational energy level) might have the opposite sign from $J(T)$ at higher temperatures. Two examples are shown in Figure 16 of such J *vs* T behavior. In either case, the *observed* coupling, $|J|$, *decreases* over a certain temperature range (designated by the solid lines) before dramatically increasing (dashed line). According to this model, *any* exchange-coupled system could, in principle, show this "inverse temperature dependence". Although plausible, this explanation does not take into account the unique feature of the particular complexes we study here: the fact that they are unsaturated. It seems likely that the unprecedented temperature dependence in these complexes is related to this distinguishing molecular feature.

Reversible Dimerization of Unsaturated Species. The large phosphine ligands in these complexes are employed to prevent dimer formation. However, halide bridges have been shown
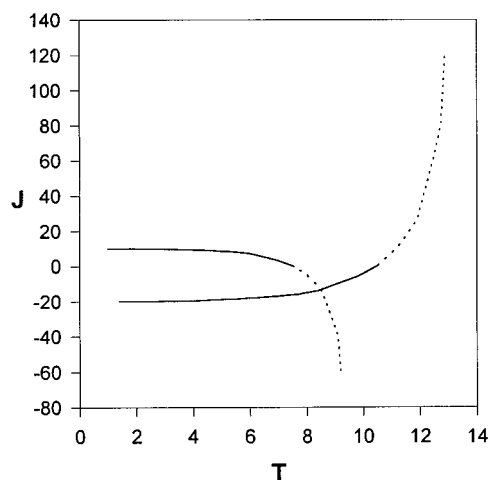
(35) Poulton, J. T.; Hauger, B. E.; Kuhlman, R. L.; Caulton, K. G. *Inorg. Chem.* **1994**, *33*, 3325.

Figure 16. Possible behavior of $J(T)$.

in similar complexes to mediate halide exchange reactions.[35] If dimerization is rapid and reversible on the NMR time scale, then an AB_2 pattern should still be observed for these trihydrides. However, the observed coupling would have contributions from both the monomeric complex and the dimeric complex, as shown in eq 12, where χ values are mole fractions and J values are

$$J_{obs} = \chi_m J_m + \chi_d J_d \qquad (12)$$

coupling constants of individual configurations (eq 13). The

$$2L_2OsH_3Cl \rightleftharpoons \{L_2OsH_3Cl\}_2 \qquad (13)$$
$$\mathbf{m} \qquad\qquad \mathbf{d}$$
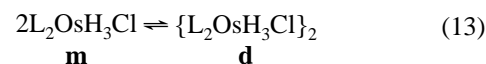
"m" subscript denotes monomeric species and "d" dimeric species. Dimerization is entropically disfavored: $\Delta S° < 0$. It follows that, with increasing temperature, χ_m increases while χ_d decreases. If $J_d > J_m$, then J_{obs} decreases as the temperature increases. The situation is complicated by the fact that both J_d and J_m are temperature-dependent and may also have opposite signs. The simplest case leading to the observed behavior is $J_m \ll J_d$, where J_d is only moderately temperature-dependent. This hypothesis is readily testable, however, since χ_m and χ_d should be dependent on the total concentration of the complex. Spectra taken with different initial concentrations of **1** (18.2 and 43.7 mM in methylcyclohexane-d_{14}) show identical spectra at three different temperatures. Thus, this model can be ruled out.

Reversible Solvent Coordination. These osmium trihydride complexes are the only known 16-electron complexes to show exchange coupling. It is perhaps more than a coincidence that they are also the only complexes to have an inverse dependence of J on T. In fact, the unsaturation may allow these complexes to undergo rapid and reversible solvent coordination (eq 14) of even weakly coordinating solvents such as methylcyclohexane.

$$L_2OsH_3X + solv \overset{K}{\rightleftharpoons} L_2OsH_3Cl(solv) \qquad (14)$$
$$\quad J_u \qquad\qquad\qquad J_s$$
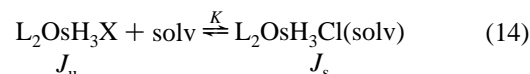
Alkane coordination is very rarely invoked, although coordination of alkanes such as methane and cyclohexane to a metal center has been observed in xenon solvent. Even that study was plagued by the challenge of spectroscopically distinguishing weak adduct binding from no binding at all.[36] An equilibrium such as that shown in eq 14 could explain the inverse temperature dependence in a similar way to the dimerization model. The same equations hold, except that the subscript "s"

(36) Bengali, A. A.; Schultz, R. H.; Moore, C. B.; Bergman, R. G. *J. Am. Chem. Soc.* **1994**, *116*, 9585.

denotes the solvent-coordinated form and "u" indicates the unsaturated complex.

Spectra of the alkoxide complex (inset in Figure 15) in three different solvents, toluene-d_8, methylcyclohexane-d_{14}, and CD$_2$-Cl$_2$, are easily explained by this model. Since alkoxide is a very good π-donor and bulkier than halides, coordination of toluene or methylcyclohexane is nearly zero; therefore, J_{obs} is almost temperature-independent in these solvents. However, J_{obs} decreases in CD$_2$Cl$_2$ (a more nucleophilic solvent) with increasing temperature, indicating coordination. In principle, the three plots would merge at the limit of no solvent coordination, and it does appear that J_{obs} in CD$_2$Cl$_2$ is approaching J_{obs} in the other solvents at higher temperatures. Unfortunately, line broadening precludes us from measuring these values at higher temperatures.

Proposals of coordination of methylcyclohexane must be very critically examined, since alkanes are not generally accepted as viable ligands. The lack of literature examples of alkane coordination may be due more to inherent difficulties in detection rather than to extreme scarcity. Let us accept, for the sake of argument, that solvent coordination is truly responsible for this inverse temperature dependence. Now, if H/H coupling of normal magnitude were present in this complex, solvent coordination would be nearly impossible to detect because the observed chemical shifts do not change appreciably with temperature. Infrared bands should be present for the solvent-coordinated complex but have only very low intensity, since the complex is still mostly in the solvent-free form. Other spectroscopic techniques would suffer similarly.

One might propose some "temperature-dependent solvent interaction" other than actual coordination of methylcyclohexane (i.e., in the first solvation sheath).[37] Once again, it is then an astounding coincidence that this interaction is absent in *all* known exchange-coupled 18-electron species, while it is present in *all* known exchange-coupled 16-electron species. It is difficult to imagine this "interaction" being anything other than coordination of a C−H bond to the metal center.

Agostic Interaction. We have considered the possibility that the unusual temperature dependence could be due to an intramolecular interaction: an agostic bond from a phosphine alkyl. Due to a negative $\Delta S°$ for agostic formation, this interaction would be favored by low temperatures and, therefore, could lead to the observed temperature dependence. However, we do not prefer this model because it does not explain the solvent dependence observed for L$_2$OsH$_3$(OR) (Figure 15). While the J vs T plots in Figure 15 are easily explained by the solvent coordination model (dichloromethane being the most nucleophilic solvent of the three), there is no reason to expect such a solvent dependence for an agostic interaction. Nonetheless, we recognize the general preference for intramolecular over intermolecular C−H bonds as ligands to a metal center and cannot categorically dismiss the possibility of some unexplained solvent effects on agostic formation.

Dynamics of H/H Site Exchange in L$_2$Os(H)$_3$ClL′ Species. In the hydride coalescence behavior of L$_2$Os(H)$_3$ClL′ species, hydride site exchange kinetic information is available. The value of k can be determined from the line width of a coalesced signal and the peak separation in the low-temperature limiting spectrum. The most accurate measurements are made when the lines are broad. Thus, for each L′, a temperature was chosen for which a broad line was observed, well within the temperature regime where L′-free **1** was not a significant contributor to the equilibrium (except toluene and methylcyclohexane). Table 5 summarizes this information ($\Delta\delta$ is the low-temperature separation in hertz of the outer hydride signals). Simply from peak

(37) Zamaraev, K. *New J. Chem.* **1994**, *18*, 3.

Table 5. Activation Energies for H−H Site Exchange in L$_2$Os(H)$_3$ClL′ Species[a]

L′	$\Delta\delta$	T	$\Delta\nu_{1/2}$	k	$\Delta G^{\ddagger}$
none, in CD$_3$C$_6$D$_5$	2160	205	310	14200	8.0
none, in CD$_3$C$_6$D$_{11}$	2153	197	830	5000	8.0
THF	1785	168	150	21000	6.3
CH$_3$OH	1078	196	520	2500	8.3
acetone	320	196	97	1200	8.6
MeCN	951	199	220	4200	8.2
NH$_3$	938	280	110	8000	11.4

[a] $\Delta\delta$ indicates the greatest peak separation in the low-temperature limiting spectrum, in hertz; T is in kelvin; $\Delta\nu_{1/2}$ is the peak width at half-height in hertz; k is in s−1; $\Delta G^{\ddagger}$ is in kcal/mol.

separations and line widths, it is clear that the rate of hydride site exchange follows the trend L′ = NH$_3$ < CH$_3$OH < THF. Spectra were simulated using DNMR5 with a single rate constant, assuming that H$_a$/H$_b$ site exchange occurs at the same rate as H$_b$/H$_c$ site exchange. While this assumption is not rigorously true, the simplification is necessary for using the DNMR5 program. Although this is an oversimplification, these k values are given for comparative purposes. Values of $\Delta G^{\ddagger}$ are calculated according to transition state theory and included in Table 5 for further discussion.

Summary of Trends for Os(H)$_3$ClL′L$_2$ Species. The data for L′ binding are summarized in Table 6. The list of L′ is given roughly in the order of their donor abilities ($\Delta H°$ of L′ binding). One *general* trend is that a better donating L′ has a lower value of J. There are exceptions, however. For example, J_{HH} of Os(H)$_3$Cl(NH$_3$)L$_2$ in CD$_2$Cl$_2$ is 150 Hz, whereas the acetone complex has J_{HH} values of 30 and 60 Hz. Also, the hydride chemical shift is generally more perturbed from that of **1** (in this case, more downfield) for the stronger donating ligands. The most consistent trend is that J seems to increase as the barrier height to hydride site exchange decreases. This is most clear in the series L$_2$Os(H)$_3$ClL′ (L′ = THF, CH$_3$OH, acetone, NH$_3$). We do not consider L′ = toluene-d_8 or CD$_3$C$_6$D$_{11}$ in this trend since we observe averaged J values in these cases. There seems to be no trend in T_{1min} values, which is evidence that exchange coupling may be more sensitive to barrier heights than H···H separations. Entropies of association are more negative for ligands with more atoms (more degrees of freedom to be lost upon coordination).

The Dynamic Computational Study. The experimental results show an extreme sensitivity of J_{ex} to the experimental conditions. Although in the theoretical study we could not simulate the influence of each different added ligand or of the several solvents that have been used, we will show how sensitive the calculated J is to the nature of the complex and how several experimental trends are well described by the dynamic study. Since the dynamic study used here is different from that of Lluch and Lledos et al.,[12a] we have presented its essential aspects. The dynamic study is focused on OsH$_3$X(PH$_3$)$_2$ (X = Cl, I) and OsH$_3$Cl(PH$_3$)$_3$.

Choice of the Reaction Coordinate. As mentioned above, the main component of the reaction coordinate is ϕ. However, other coordinates can also participate. An analysis of the frequencies in the ground and transition states provides an indication of the variables to consider in the dynamic study. The determination of the frequencies (calculated in the case of coupling of ϕ and r) for the Cl case shows that the H···H vibration, k_{rr}, has a higher frequency in the ground state (1521 cm^{-1}) than in the transition state (1435 cm^{-1}). Similar values are found for the six-coordinate iodide but are lowered in the seven-coordinate chloride species (1474 for $\phi = 0°$ and 1393 cm^{-1} for $\phi = 90°$). This confirms the idea that the 18-electron complex is more fluxional, and it stresses the importance of r

Table 6. Summary of Observations for $L_2Os(H)_3ClL'$ Complexes[a]

L'	δ	J/T	spin system	ΔS°	ΔH°	ΔG‡	T_{1min}/T
toluene-d_8	−19	920/−110	AB_2			8.0	72/−70
$CD_3C_6D_{11}$[c]	−19	670/−100	AB_2			8.0	78/−70
THF[d]	−15	320/−114	ABX	−33(1)	−5.8(2)	6.3	
CH_3OH[e]	−15	55, 73/−99	ABC	−25.5(3)	−6.66(8)	8.3	70/−66
CH_3OD[f]	−15	70/−99	ABX				<84/−66
CH_3OH[b]	−15		AMX				<79/−66
acetone[e]	−14	30, 60/−89	ABC	−41.8(5)	−10.4(1)	8.6	65/−77
CH_3CN[e]	−12		AM_2	−14.7(9)[h]	−17.6(3)[g]	8.2	82/−55
$(CH_3CN)_2^+$ [e]	−12	J_{HD} = 2.80/25	A_3				66/−99
NH_3[b]	−13	12, 25/−78	ABC	−16(1)[h]	−20.7(3)[g]	11.4	55/−76
NH_3[e]	−13	150/−68	ABX				<64/−77
$(NH_3)_2^+$ [e]	−13	25/−68	AB_2				81[i]/−66
PEt_3[e]	−12		AM_2				78[i]/−68

[a] The averaged chemical shift of the hydride resonances is represented by δ. Units are as follows: δ, ppm, J, Hz; T, °C; ΔH°, kcal/mol/ ΔS°, cal/(mol K); ΔG‡, kcal/mol; T_{1min}, ms at 300 MHz. [b] Toluene-d_8. [c] Methylcyclohexane-d_{14}. [d] THF-d_8−toluene-d_8 (7/3). [e] CD_2Cl_2. [f] THF-d_8−toluene-d_8 (9/1). [g] Estimated from ΔH‡ for L' dissociation. [h] Estimated from ΔS‡ for L' dissociation. [i] Weighted average from the two signals observed at the T_{1min} temperature.

in the dynamic study. It also suggests that there is no formation of a dihydrogen ligand in the transition state, since then the H···H vibrational frequency should have been higher than in the ground state. The study of the coupling of other variables shows that the lowest frequency for φ = 0° or 90° corresponds to k_{rr} and that all other frequencies are significantly higher. The coupling of θ with r is negligible, which is not the case for the coupling of r and z. This preliminary study establishes that the dynamic study should focus on the variables φ and r. The dynamic study, described in the computational details section, was thus carried out using three sets of variables, {φ,r}, {φ,r,θ} and {φ,r,z}, for the case of the six-coordinate chloride and using only the first set for the case of the six-coordinate iodide and the seven-coordinate chloride species.

Vibrational Levels for $OsH_3Cl(PH_3)_2$. (a) Symmetry Properties of the Wave Functions. Relation with Effective Coupling J_n. The permutation inversion group for two atoms 1 and 2 is S_2*, which has four symmetry operations: E, the identity; (1,2), the permutation of 1 and 2; and the coupling of the two previous operations with the inversion of these particles with respect to the center of mass, which are noted $E*$ and $(1,2)*$. The variable φ transforms as φ, π + φ, −φ and π − φ under the previous symmetry operations. This allows the determination of a symmetry-adapted basis set. Since the S_2* group is isomorphic to C_{2v}, the symmetry-adapted basis sets are labeled A_1 (symmetric with respect to both operations), B_2 (symmetric with respect to φ → −φ and antisymmetric with respect to φ → π + φ), B_1 (antisymmetric with respect to φ → −φ and symmetric with respect to φ → π + φ), and A_2 (antisymmetric with respect to both operations). In the absence of tunneling, the A_1 and B_2 levels on one side and the A_2 and B_1 levels on the other side would be degenerate. Tunneling destroys the degeneracy within each (A_1,B_2) or (A_2,B_1) pair. Furthermore, each of the nuclear levels is associated with a given nuclear spin function. Since the total wave function is antisymmetric with respect to exchange of particles, the triplet nuclear spin is associated with an A_1 or B_1 level, while the singlet nuclear spin is associated with the B_2 or A_2 level. Following the theory presented by Zilm, transitions occur within these pairs, and the effective J_n for each pair of levels is directly the difference in energy between the two levels of a given pair. The determination of the symmetry of the wave function for each level thus allows a clear association between the NMR transition and the nature of the levels.

(b) The Energy Levels for the {φ,r} Variables. Energy levels have been calculated much higher than the top of the barrier in order to have accurate values of the levels below the barrier. However, only the levels below the barrier have been included in the calculation of J(T). (Other selection criteria have

Table 7. Vibrational Levels (cm^{-1}) for $OsH_3Cl(PH_3)_2$ from the {φ,r} Basis Set[a]

n	E_n (cm^{-1})	J_n (Hz)	p_n^+	$p_n^+J_n$ (Hz)
1	886	32	0.4128	13
2	1216	-9.55×10^2	0.75710×10^{-1}	−72
3	1610	1.81×10^4	0.1001×10^{-1}	181
4	2023	-2.78×10^5	0.1198×10^{-2}	−333
5	2438	3.37×10^6	0.1426×10^{-3}	481
6	2536	2.62×10^5	0.8601×10^{-4}	22
7	2838	-2.60×10^7	0.1828×10^{-4}	−475
8	2916	-1.48×10^7	0.1225×10^{-4}	−181
9	3240	2.37×10^8	0.2313×10^{-5}	548
10	3342	1.63×10^8	0.1373×10^{-5}	224
11	3641	-2.23×10^9	0.2949×10^{-6}	−658
12	3775	-1.19×10^9	0.1479×10^{-6}	−176
13	4029	1.79×10^{10}	0.4012×10^{-7}	718
14	4204	7.42×10^9	0.1633×10^{-7}	121
15	4362	1.59×10^8	0.7277×10^{-8}	1
16	4397	-1.19×10^{11}	0.6071×10^{-8}	−722
17	4622	-4.16×10^{10}	0.1907×10^{-8}	−79
18	4731	6.30×10^{11}	0.1092×10^{-8}	688
19	4778	-4.26×10^9	0.8550×10^{-9}	−4
20	5008	-2.35×10^{12}	0.2620×10^{-9}	−616
21	5025	2.35×10^{11}	0.2400×10^{-9}	56

[a] The E_n given is that of the lower state within each doublet. The splittings, J_n (in hertz), are those between the antisymmetric (E_n^-) and the symmetric (E_n^+) states; level populations (p_n^+) of the state E_n^+ and also the contribution (hertz) of each doublet to the final J_{ex}, all at 280 K.

been studied here, but they do not significantly change the overall results.) It should be noted that the top of the barrier used as the threshold in this part has been corrected for the first vibrational levels in the ground state and the transition state. This correction gives an activation threshold energy of 5228 cm^{-1} in the case of $OsH_3Cl(PH_3)_2$.

The splittings of the levels are given in Table 7. The coupling constant associated with each level is reported as $J_n = (E_n^- - E_n^+)$, in which n is the increasing quantum number associated with each pair of levels and where E_n^- represents the energy of the level associated with the singlet nuclear spin and E_n^+ represents the level associated with the triplet nuclear spin. The sign of J_n can be either positive or negative, in contrast to other studies of quantum exchange. This comes from the explicit consideration of the symmetry property of the wave function for each energy level. For the four lowest levels, there is alternation of sign, since a pair of (A_1,B_2) levels is followed by a pair of (A_2,B_1) levels. This corresponds to a steady increase in only the quantum number associated with the variable φ. At the fifth level, the energetically higher vibrational levels associated with r start to mix in and destroy the regularity in sign alternation. Notably, it also diminishes the value of the
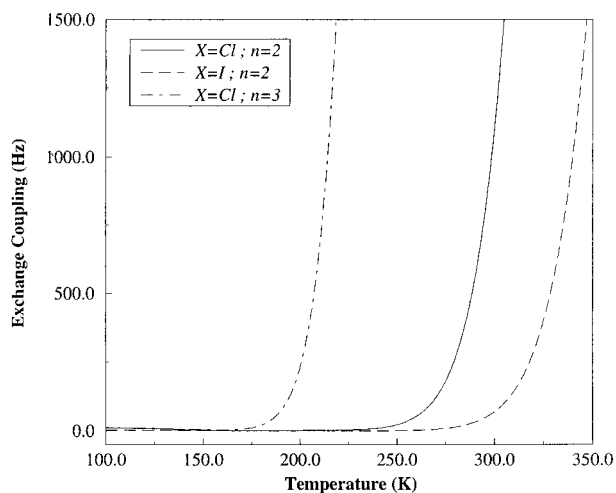
Figure 17. Calculated quantum coupling $J(T)$ for $OsH_3X(PH_3)_2$ (X = Cl, I) and for $OsH_3Cl(PH_3)_3$.

splitting. Thus, putting energy in the vibrational mode r (quantum number ν) diminishes the splitting with respect to a level of comparable energy where the rotational mode is mostly excited (compare the sixth ($\nu = 0$) and seventh levels ($\nu = 1$)). This shows the dominating influence of the rotational mode on the tunneling and thus on quantum exchange. Since the rotational mode is much softer than the vibrational mode, the quantum number in ϕ increases more rapidly than the quantum number in r as one approaches the top of the barrier. This leads to inclusion of large J_n values in $J_{ex}(T)$ when T increases.

(c) Calculation of $J_{ex}(T)$ in the Case of Variables $\{\phi,r\}$ for $OsH_3Cl(PH_3)_2$. A Boltzmann average of the individual J_n as a function of T has been carried out to obtain $J_{ex}(T)$. The sign of J_n is considered in the summation process, and the absolute value of $J_{ex}(T)$ is shown in Figure 17. The solid line corresponds to using the calculated energy barrier in the case of $OsH_3Cl(PH_3)_2$ ($V_0 = 12.9$ kcal·mol^{-1}). J_{ex} increases considerably above a temperature threshold T_0, and values much larger (1000 Hz) than those which could be observed in the case of a Fermi contact coupling (e.g., 10 Hz for nonbonded H centers) are reached. For temperatures below the threshold T_0, J_{ex} is essentially null. These results agree with behavior normally expected for J_{ex}: very small at low T and rapidly increasing with T.[38]

The population of each level[39] and the associated population weighted ($p^+{}_nJ_n$) are given in Table 7. While there is a rapid decrease in the population of each level as the energy of the level goes up, the weighted $p^+{}_nJ_n$ varies in a different manner. Due to the large value of J_n at high energy, the contribution of individual $p^+{}_nJ_n$ at high energy to the total $J_{ex}(T)$ is important. As a consequence, all levels contribute to the value of J_{ex}. J_{ex} "samples" a broad range of the potential function $V(\phi)$ and is thus very sensitive to its entire shape, not merely to the barrier height or to the first vibrational level.

(d) The Other Variables, $\{\phi,r,\theta\}$ and $\{\phi,r,z\}$. The same type of calculations were carried out with the other variables, $\{\phi,r,\theta\}$ and $\{\phi,r,z\}$. The heights of the barriers corrected for lower level frequencies (6297 and 6035 cm^{-1}, respectively) are slightly higher than those in the case of $\{\phi,r\}$ since more vibrational modes are introduced. The values of J_n are approximately equal to the values of J_n for the two-variable calculation. The inclusion of the variable θ has the least influence (it actually slightly decreases J_{ex}), while the inclusion

of z is more effective in increasing J_{ex}. This leads to a behavior of $J_{ex}(T)$, which is very close to the two-variable case, with a shift of about 20° in the temperature threshold. At very high temperature, the three sets of variables give essentially the same results. Thus, in contrast to some current propositions, the displacement of the two hydrogens *away* from the metal has no large influence on the tunneling effect and is not, at least in these systems, one of the leading components of the occurrence of NMR quantum exchange.[8,10a]

Influence of the Nature of the Halide, I *vs* Cl. A study similar to the previous case, limited to the two-variable $\{\phi,r\}$ model, was carried out for $OsH_3I(PH_3)_2$. The barrier height, corrected for the lower vibrational levels, is 5828 cm^{-1}, which is higher than that for Cl. As a result, the splitting of each corresponding level is smaller, and the resulting $J_{ex}(T)$ has a shape similar to that of Cl but shifted by nearly 100° to higher temperature (Figure 17). Thus, in agreement with experimental results, $J_{ex}(T)$ is smaller at any T in the case of I than in the case of Cl. This result illustrates the exceptional sensitivity of J_{ex} to the barrier height, as observed in all previous studies.

16- *vs* 18-Electron Complex. The barrier height in $OsH_3Cl(PH_3)_3$, corrected for the lowest vibrational frequencies, is 4129 cm^{-1}, which is significantly lower than that for $OsH_3Cl(PH_3)_2$ (5228 cm^{-1}). This leads to a significant increase in $J_{ex}(T)$ for the seven-coordinate species (Figure 17). The curve for the 18-electron species shifts to a lower temperature by approximately 100°. It is important to note that the increase in the barrier width (Figure 13) could have had the opposite result. In fact, the splitting of the lowest level is smaller for the seven-coordinate species (26 Hz *vs* 32 in the six-coordinate species). However, the lowering of the barrier already dominates at the next level, since the next splittings are −2897 and −955 Hz for the 18- and 16-electron species, respectively. Quantitative comparison of the $J_{ex}(T)$ values calculated with those for the PEt$_3$ adduct reported here is not to be pursued since the steric effects are not accounted for in our PH$_3$ model calculations.

It should not, however, be concluded that J_{ex} should be large in all 18-electron species since, for instance, the saturated Re-(NO)(CO)H$_2$L$_2$ species does not show any quantum exchange coupling.[40] The ease of H site exchange controls the occurrence of J_{ex} and, while site exchange *is* present in the Re complex, it has a higher barrier.

Comparison of the Experimental and Calculated J_{ex}. From the experimental studies on OsH_3XL_2 in "solvents", it was proposed that the unprecedented decrease of J_{ex} with increased temperature is due to an equilibrium between the unsaturated 16-electron species and a saturated, solvated complex. The theoretical study supports this interpretation. Central to the rationale of this behavior is the fact that the H site exchange barrier is lower for the solvated complex. This factor seems to dominate over all other changes caused by the solvation. However, an attempt to neglect other criteria can lead to significant misinterpretations. In particular, the width of the barrier for site exchange could be important. The change in the barrier width with the metal has been discussed in CpML-(H)$_3$+.[15] Moreover, it has been recently suggested that enzymatic H-transfer reactions involving tunneling may optimize not only barrier height but also width.[41] What is still lacking is a qualitative understanding of this factor in terms of chemical concepts. In a study parallel to this one, we have suggested that the number of permutation operations relating the two identical structures involved in the tunneling could be important. In other words, the barrier width is related to the displacement

(38) Heinekey, D. M.; Hinkle, A. S.; Close, J. D. *J. Am. Chem. Soc.* **1996**, *118*, 5353.

(39) The populations $p^-{}_n$ and $p^+{}_n$ of $E^-{}_n$ and $E^+{}_n$, respectively, are essentially equal. Thus, only one value, $p^+{}_n$, was used.

(40) Bakhmutov, V.; Bürgi, T.; Burger, P.; Ruppli, U.; Berke, H. *Organometallics* **1994**, *13*, 4203.

(41) Jonsson, T.; Glickman, M. H.; Sun, S.; Klinman, J. P. *J. Am. Chem. Soc.* **1996**, *118*, 10319.

10168   *J. Am. Chem. Soc., Vol. 119, No. 42, 1997*

Kuhlman et al.

of atoms between the ground state and the transition state for H exchange. It thus can happen that increasing the number of atoms in the molecule could lead to displacement of more atoms during site exchange and thus lower J_{ex}, even if the activation energy remains low. This could partially account for the small J_{ex} observed for X = OCH_2CF_3. Likewise, the slight increase in the barrier width in the seven-coordinate solvated species may become important for some specific ligand. J_{ex} is sensitive to all aspects of the potential energy surface. It could become a very sensitive spectroscopic probe and has already been used here for detection of very weak coordination to the metal center.

Conclusions

The reactivity of complexes **1**−**4** ranges from room-temperature dehydrogenation of methanol, yielding $L_2OsHCl(CO)(H_2)$, to proposed low-temperature coordination of C−H bonds. The ability of **1** to bind *ligands* which are traditionally considered *solvents* was extensively investigated. The binding enthalpies for five different σ-donating ligands show the trend NH_3 > MeCN > acetone > MeOH > THF.

Nonoctahedral dihydrogen complexes are rare, and their rich chemistry is demonstrated here. Unlike similar species, some of the fluxional processes in these complexes can be slowed, and that property has allowed us to draw several conclusions: (1) L' adds *cis* to X in L_2OsH_3X and (2) exchange coupling is often detected between only two hydrides in trihydride complexes of spin system ABC. The hypersensitivity of exchange coupling is employed to detect the formation of hydrogen bonds and weak solvent coordination.

$L_2Os(H)_3Cl$ shows strong contrast in its reactivity with CO (which causes reductive coupling of $2H^- \rightarrow H_2 + 2e$, followed by loss of H_2) and with MeCN or NH_3 (which cause loss of Cl^-, which is then replaced by MeCN or NH_3, respectively). This can be rationalized by the π-acidity of CO causing H_2 formation, while $L_2Os(H)_3ClL'$ (L' = MeCN or NH_3) is a trihydride, with a chloride which can dissociate ionically when encouraged by hydrogen bonding and a polar solvent.

Much remains to be understood in the theory and calculations of quantum exchange. Among them are the role of the third hydride, the path length, and the inclusion of more atoms in the calculation of energy levels. The role of the third hydride has never been considered since the pairwise exchange is thought to dominate. Would successive pairwise exchange be influential? No calculations have been carried out for a concerted cyclic permutation of the three H's. Such a study would require further development of the NMR quantum exchange theory. The path length and the role of all other atoms in the molecules are also of interest. In contrast to previous studies, our path did not start with a decrease of the H···H distance prior to rotation. Our study shows that this constraint is not necessary for obtaining reasonable values of *J*. However, more comparisons between the two methods would be useful.

Finally, is quantum exchange of any interest besides an exotic phenomenon limited to an extremely small set of metal hydrides? For the moment, the high sensitivity of J_{ex} to all aspects of the nature of the complex makes its occurrence still a challenge for predicting which molecules will display quantum exchange. However, in the case where a full understanding of it could be made, this can be used as an ultrasensitive measurement of the characteristics of the complex. In the present case, it can be used for detecting the presence of even weak additional coordination to the 16-electron complex, even in the case where other techniques of detection would fail. There is, hopefully, future use for this phenomenon.

Experimental Section

All reactions and manipulations were conducted using standard Schlenk and glovebox techniques. Solvents were dried and distilled under argon and stored in air-tight solvent bulbs with Teflon closures. All NMR solvents were dried, vacuum-transferred, and stored in a glovebox. Complexes $(P^iPr_3)_2Os(H)_3X$ (X = Cl, I) were synthesized according to published procedures.[17] Proton NMR spectra were obtained on a Varian XL-300 or a Bruker AM 500 spectrometer, while ^{31}P NMR spectra were recorded on a Nicolet 360 MHz instrument. All T_1 measurements were made at 300 MHz using the inversion−recovery method and Varian software. Chemical shifts were referenced to residual protio solvent peaks (^1H) or external H_3PO_4 (^{31}P). Temperatures were standardized according to the peak separation of CH_3-OH; temperatures below −100 °C require extrapolation and are less reliable. Infrared spectra were recorded on a Nicolet 510P FT-IR spectrometer.

$(P^iPr_3)_2Os(H)_3(OCH(CF_3)_2)$ (4). This complex was prepared in an NMR tube by metathesis of **1** with 1 equiv of $Tl(OCH(CF_3)_2)$. ^1H NMR (toluene-d_8) at 20 °C, δ 4.82 (sept, J_{HF} = 6.5 Hz, 1H), 1.89 (mult, 6H), 1.07 (app q, N = 7.6, 36H), −19.07 (br, 3H); at 60 °C, −18.95 (t, J_{HP} = 11.3 Hz); at −83 °C, −16.00 (tt, J_{HH} = 50.7 Hz, J_{HP} = 10.3 Hz), −20.77 (dt, J_{HH} = 50.7 Hz, J_{HP} = 11.6 Hz). $^{31}P\{^1H\}$ NMR (toluene-d_8): at 20 °C), δ 53.7 (s); at −80 °C, 55.8 (d, J_{PP} = 274 Hz), 51.2 (d, J_{PP} = 274 Hz).

$(P^iPr_3)_2Os(H)_3(OCH_2CF_3)$ (5). Metathesis of **1** with $TlOCH_2CF_3$ yields this complex. ^1H NMR (toluene-d_8): at 20 °C, δ 4.67 (q, J_{HF} = 9.4 Hz, 2H), 1.89 (mult, 6H), 1.08 (app q, N = 6.7, 36H), −18.4 (br, 3H); at −70 °C, −15.13 (br t, J_{HH} = 34 Hz), −19.90 (dt, J_{HH} = 34 Hz, J_{HP} = 13 Hz). $^{31}P\{^1H\}$ NMR (toluene-d_8): at 20 °C, δ 52.3 (s).

Formation of L_2OsH_3ClL' Complexes (General). In an argon-filled glovebox, a glass vial was charged with **1** (ca. 10 mg). A separate vial was charged with L' in cases where L' is a solid or liquid. The masses of the two species were determined to within ±0.1 mg. The L' was then dissolved in the indicated NMR solvent and pipetted into the vial containing **1**. In cases where thermodynamic measurements were made, requiring known concentrations, liquids were added via microsyringe. The final volume was determined by using a calibrated NMR tube. The resulting solution was transferred to an NMR tube. In cases where L' = NH_3 or CO, an NMR tube with a Teflon closure was employed, and the gas was introduced after three freeze−pump−thaw cycles. Product isolation was generally not feasible due to facile loss of L'.

$(P^iPr_3)_2Os(H)_3Cl(PEt_3)$. $^{31}P\{^1H\}$ NMR (CD$_2$Cl$_2$): δ 18.7 (d, J_{PP} = 16 Hz, 2P), −23.7 (t, J_{PP} = 16 Hz, 1P). ^1H NMR (CD$_2$Cl$_2$): δ 2.48 (mult, 6H), 2.17 (app quint, J = 6.6 Hz, 6H), 1.5−1.2 (several overlapping, 45H), −12.2 (br, 3H); at −80 °C, −6.3 (dt, J_{HP} = 71 Hz, J_{HP} = 21 Hz, 1H), −15.04 (br, 2H). T_1 measurements (toluene-d_8): −68/81, 76; −90/132, 81, °C/ms for δ −6, −15.

$(P^iPr_3)_2Os(H)_3Cl(NH_3)$. $^{31}P\{^1H\}$ NMR (toluene-d_8): δ 26.2 (s). ^1H NMR (toluene-d_8): δ 2.25 (s, 3H), 2.06 (mult, 6H), 1.18 (apparent q, N = 6.5, 18H), 1.18 (apparent q, N = 6.0, 18H), −13.21 (br, 3H); at 64 °C, −13.38 (t, J_{HP} = 12.8 Hz); at −69 °C, −11.33 (dt, J_{HH} = 26 Hz, J_{HP} = 13 Hz, 1H), −14.30 (mult, 1H), −14.48 (dt, J_{HH} = 13 Hz, J_{HP} = 11 Hz, 1H); at −68 °C (CD$_2$Cl$_2$), −11.63 (br d, J = 150 Hz, 1H), −14.14 (br d, J = 150 Hz, 1H), −14.89 (br s, 1H). T_1 measurements (toluene-d_8): −66/85, 77, 88; −77/59, 47, 61 °C/ms for δ −11, −14, −14.4.

$(P^iPr_3)_2Os(H)_3(NH_3)_2{}^+$. $^{31}P\{^1H\}$ NMR (CD$_2$Cl$_2$): δ 25.5 (s). ^1H NMR (CD$_2$Cl$_2$): δ 3.64 (s, 6H), 2.08 (mult, 6H), 1.14 (apparent q, N = 6.5, 36H), −12.89 (t, J_{HP} = 12.3 Hz, 3H); at −68 °C, −12.70 (dt, J_{HH} = 25 Hz, J_{HP} = 13 Hz, 2H), −13.63 (mult, 1H). T_1 measurements: −55/86, 79; −66/84, 75; −77/98, 71; −87/114, 82 °C/ms for δ −12.7, −13.6.

$(P^iPr_3)_2Os(H)_3Cl(MeCN)$. $^{31}P\{^1H\}$ NMR (toluene-d_8): δ 26.8 (s). ^1H NMR (toluene-d_8): δ 2.30 (mult, 6H), 1.26 (apparent q, N = 6.4, 36H), 1.08 (s, 3H), −12.69 (t, J_{HP} = 13.1 Hz, 3H); at −90 °C (toluene-d_8), −10.30 (br, 1H), −13.50 (br, 2H). T_1 measurements: −24/105; −35/89, −46/82; −57/82; -68/105 °C/ms.

$(P^iPr_3)_2Os(H)_3Cl(acetone)$. At room temperature in CD$_2$Cl$_2$, signals are observed for **1** and acetone. Selected ^1H NMR (CD$_2$Cl$_2$, −89 °C): ABC pattern, δ −12.92 (A), −13.70 (B), −14.01 (C) (J_{AB} = 60 Hz, J_{AC} = 0 Hz, J_{BC} = 30 Hz). T_1 measurements: −77/65; −67/73 °C/ms.

Table 8.   Crystallographic Data for [Os(H)₃(NH₃)₂(P^{i}Pr₃)₂]Cl

formula	C₁₈H₅₁ClN₂OsP₂	fw	583.25
a	11.561(4) Å	space group	P1̄
b	14.215(5) Å	T	−171 °C
c	8.851(3) Å	λ	0.710 69 Å^a
α	97.51(2)°	r$_{calc}$	1.481
β	107.73(2)°	m	51.0
γ	104.47(2)°	R(F$_o$)^b	0.0416
V	1307.49 Å³	R$_w$(F$_o$)^c	0.0426

^{a} Graphite monochromator. ^{b} $R = \sum ||F_o| - |F_c||/\sum |F_o|$. ^{c} $R_w = [\sum w(|F_o| - |F_c|)^2/\sum w|F_o|^2]^{1/2}$, where $w = 1/\sigma^2(|F_o|)$.

(P^{i}Pr₃)₂Os(H)₃Cl(CH₃OH). At room temperature in CD₂Cl₂, ¹H NMR signals are observed for **1** and CH₃OH. ¹H NMR (CD₂Cl₂) at −98 °C), δ 4.82 (1H), 3.68 (3H), 2.23 (6H), 1.30 (36H); at −108 °C, −13.23 (d, J = 55 Hz), −14.71 (apparent triplet, outerline separation = 130 Hz), −16.82 (d, J = 73 Hz). Selected ¹H NMR (toluene-d₈, −89 °C): δ −13.06 (br), −14.70 (br), −16.50 (br). Selected ¹H NMR (THF-d₈, −98 °C): δ −12.47 (d, J = 70 Hz), −14.88 (d, J = 70 Hz), −16.97 (s). T₁ measurements (CD₂Cl₂): −77/72; −67/70; −56/77 °C/ms.

(P^{i}Pr₃)₂Os(H)₃Cl(THF-d₈). At room temperature, the spectra of **1** in THF-d₈ are essentially the same as those in toluene-d₈. Selected ¹H NMR (THF-d₈/toluene-d₈ (7:3), −113 °C): δ −12.2 (d, J = 320 Hz, 1H), −15.0 (d, J = 320 Hz, 1H), −17.8 (s, 1H).

X-ray Structure Determination. A crystal of suitable size was mounted in a nitrogen atmosphere glovebag using silicone grease. It was then transferred to a goniostat where it was cooled to −171 °C for characterization (Table 8) and data collection (6° < 2θ < 50°). A preliminary search revealed a triclinic cell. An initial choice of space group P1̄ was later proven correct by the successful solution of the structure. After complete intensity data collection, a correction was made for a drift in the data as well as for absorption (transmission factors ranged from 0.47 to 0.69). The drift correction was based on the change in four standards (0 6 0, 3 0 0, 0 0 −4, and 2 2 −4) which had been measured every 300 data. Data processing then produced a unique set of 4623 intensities and a residual of 0.031 for the averaging of 705 reflections which had been measured more than once. The structure was solved by a combination of direct methods (MULTAN78) and Fourier techniques. The position of the osmium atom was obtained from an initial E-map. The positions of the remaining non-hydrogen atoms were obtained from iterations of a least-squares refinement followed by a difference Fourier calculation. Only a few of the hydrogen atoms were found, and none of the anticipated hydride ligands on the osmium could be detected above the background noise. The hydrogens bonded to carbon and nitrogen were included in fixed calculated positions with thermal parameters fixed at 1 plus the isotropic thermal parameter of the atom to which the hydrogen was bonded. The hydride ligands were not included in the refinement of the structure but are included in the chemical formulas and in other calculations such as for the density and linear absorption coefficient. In the final cycles of refinement, the non-hydrogen atoms were varied with anisotropic thermal parameters. The largest peaks in the final difference map were osmium residuals in the range 1.1−2.5 e/Å³, and, as noted above, none were in chemically reasonable positions to be the hydride ligands. All other residual peaks were 0.8 e/Å³ or less. The deepest hole was −1.34 e/Å³. The results of the structure determination are given in Table 7, in Figure 10, and as Supporting Information.

Computational Details. The model systems are OsH₃XL₂ (X = Cl, I, OH; L = PH₃, PMe₃). The full study was done for the two halides and PH₃ as a model phosphine. The study for X = OH and L = PMe₃ was limited to some selected structures. Effective core potential *ab initio* calculations at the MP2 level were carried out. Details have been given previously.[13]

In the dynamic study, the calculation of the splittings is equivalent to computing the vibrational energy levels associated with those internal coordinates which have been selected; e.g., if we consider the (φ,r,z) coordinates as defined in the body of the text, the corresponding Hamiltonian operator is

$$H = -\frac{\hbar^2}{2\mu r^2}\frac{\partial^2}{\partial\phi^2} - \frac{\hbar^2}{2\mu}\frac{1}{r}\frac{\partial}{\partial r}r\frac{\partial}{\partial r} - \frac{\hbar^2}{2m_{H_2}}\frac{\partial^2}{\partial z^2} + V(\phi,r,z)$$

The Hamiltonian is that of a planar rotor (φ,r) moving in a plane along the z direction. If only the (φ,r) coordinates are relevant, the ∂²/∂z² term vanishes in the above expression. The potential has been described by singling-out a reaction coordinate and expressing the effective potential along that coordinate by assuming the other degrees of freedom to be adiabatic, following the pioneering work of Truhlar and Kuppermann[42] and the more general procedures of the reaction path Hamiltonian.[43] More specifically, for a fixed φ value, the potential is expanded in power series of r and z around their local equilibrium values.

The vibrational energy levels correspond to the eigenvalue of the above Hamiltonian in some appropriate basis set. In order to diagonalize efficiently this operator, we have made use of the successive adiabatic reduction method of Bacic and Light.[44] An adiabatic (r,z) basis set with respect to the variable φ is defined in order to contract as much as possible the overall basis set. The permutation symmetry, as described in the text, has been built into the diagonalization scheme. One can show that the symmetry-adapted bases for the φ motion are the following:

A_1:   {cos(2kφ), k = 0, ···, N}

A_2:   {sin(2kφ), k = 1, ···, N}

$B1$:   {cos(2k + 1)φ), k = 1, ···, N}

B_2:   {sin(2k + 1)φ), k = 1, ···, N}

Supporting Information Available: Rate and equilibrium data, full crystallographic data including anisotropic thermal parameters, and Eyring plots of kinetic data, (11 pages). See any current masthead page for ordering and Internet access instructions.

JA970603J

(42) Truhlar, D. G.; Kuppermann, A. *J. Am. Chem. Soc.* **1971**, *93*, 1840.
(43) (a) Miller, W. H. *J. Chem. Phys.* **1980**, *72*, 99. (b) Garret, B. C.; Truhlar, D. G. *Proc. Natl. Acad. Sci. U.S.A.* **1979**, *76*, 4755. (c) Brown, F. B.; Tucker, S. C.; Truhlar, D. G. *J. Chem. Phys.* **1985**, *83*, 4451. (d) Hancock, G. C.; Rejto, P.; Steckler, R.; Brown, F. B.; Schwenke, D. W.; Truhlar, D. G. *J. Chem. Phys.* **1986**, *85*, 4997.
(44) (a) Light, J. C.; Hamilton, I. P.; Lill, J. W. *J. Chem. Phys.* **1985**, *82*, 1400. (b) Lill, J. V.; Parker, G. A.; Light, J. C. *J. Chem. Phys.* **1986**, *85*, 900. (c) Bacic, Z.; Light, J. C. *J. Chem. Phys.* **1986**, *85*, 4594. (d) Bacic, Z.; Light, J. C. *J. Chem. Phys.* **1986**, *86*, 3065. (e) Bacic, Z.; Light, J. C. *J. Chem. Phys.* **1987**, *87*, 4008.